

Design and development of Patterned shape memory Alloy thin Film

A Thesis

*Submitted in partial fulfillment of the
requirements for the award of the degree*

of

Master of Technology

in

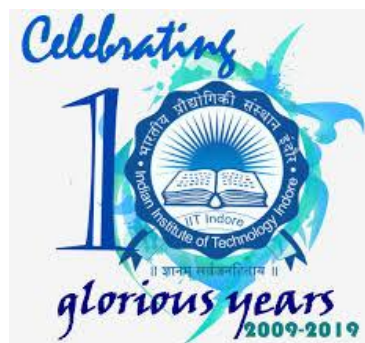
Mechanical Engineering

With specialization in

Production and Industrial Engineering

By

Ankit Kaithwas



**Discipline of Mechanical Engineering
Indian Institute of Technology Indore
JUNE 2019**

Candidate's Declaration

I hereby certify that the work which is being presented in the thesis entitled "**Design and development of patterned shape memory alloy thin films**" in the partial fulfillment of the requirements for the award of the degree of **Master of Technology in Mechanical Engineering** with specialization in **Production and Industrial Engineering** are submitted in the **Discipline of Mechanical Engineering, Indian Institute of Technology Indore**, is an authentic record of my own work carried out during the time period from **May 2018 to June 2019** under the supervision of **Dr. I.A.Palani** of Discipline of Mechanical Engineering. The matter presented in this thesis has not been submitted by me for the award of any degree from any other institute.

Ankit Kaithwas

This is to certify that the above statement made by the candidate is correct to the best of our knowledge.

(Dr. I.A. Palani)

Ankit Kaithwas has successfully completed his M.Tech Oral Examination held on

Signature of M.Tech Thesis Supervisors

Date:

Signature of PSPC member 1:

Date:

Signature of Convener, DPGC

Date:

Signature of PSPC member 2:

Date:

ACKNOWLEDGMENT

I take this opportunity to express my deep sense of respect and gratitude towards Dr. I.A. Palani for believing in me to carry out this work under his supervision. His constant encouragement and constructive support have enabled this work to achieve its present form. His innovative perspective towards things and his continuous pursuit for perfection has had a profound effect on me and has transformed me majorly. I feel great privileged to be one of his students.

My gratitude is also extended towards my PSPC members Dr. Vipul Singh and Dr. Yuvraj Kumar Madhukar for their guidance and cooperation.

I also express my sincere thanks to Sophisticated Instrumentation Centre(SIC), IIT indore for providing me with the necessary characterization facility throughout my research period.

I express my deep sense of gratitude to PhD scholars Jayachandran S, Karthick S, Mani Prabhu S S, Manikandan M, Rajagopalan P, Nandini Patra, Suhel Khan and Muralitharan M for bearing with me and always maintaining a homely atmosphere in the lab.

I am thankful to IIT indore for giving me an opportunity to carry out the research work and providing all the facilities. Very special thanks to Prof.Pradeep Mathur, Director, IIT Indore, for supporting and providing us facilities to perform my work smoothly here.

Special thanks are extended to my colleagues Shivam Mishra, Gaurav Deshwal, Vinod Singh Thakur, Shalini Singh, Mayank Sharma for their help and suggestions whenever I needed and for always giving me company. I am also thankful to Lab staff of Mechanical Engineering Labs and Central Workshop for their cooperation.

ANKIT KAITHWAS

*Dedicated to my Guide
my family
&
my friends*

Abstract

The research studied focuses on the development of patterned CuAlNi SMA bimorph on prestrained Kapton polyimide substrates. A flexible substrate such as Kapton polyimide is appropriate for obtaining a two-way memory effect. Shape memory alloy was deposited on a 75 μ m thick Kapton polyimide substrate. A patterned structure was fabricated in a planar fully deposited bimorph by means of laser fabrication method. Using electrical actuation configuration through Joule heating, the displacement of distinct patterns was explored at different voltages and different frequencies ranging from 1V to 4V and 0.25Hz -0.50 Hz respectively. The forward movement was accomplished by shape memory alloy effect and the return movement was due to the impact of Kapton polyimide substrate. Comparison of distinct patterns with the planar fully deposited has been done. The maximum displacement of 4.10 mm was investigated in a Deltoid patterned bimorph at 3V. The Shape Recovery Ratio of distinctly patterned bimorph was also investigated. The Austenite start temperature A_s and Austenite finish temperature A_f was found to be 233.2 and 234.5 in $^{\circ}$ C respectively. furthermore, the morphological, structural and thermal behavior of the SMA bimorph was investigated in detail.

List of publications:

- Jayachandran S, **AnkitKaithwas**, Brolin, Manikandan M, AkashK, SachinBhirodkar, I.A.Palani. (**Investigation on effects of patterned NiTi Shape Memory Alloy (SMA) thin film on actuation characteristics.**) Recent Innovations in Advanced Materials (RIAM) - (18th-19th September 2018)
- Jayachandran S, Brolin, HariVishanth, **AnkitKaithwas**, Manikandan M, AkashK, I.A.Palani. (**Actuation Study of Copper Based patterned SMA bimorph**). ISSS National Conference on MEMS smart materials 2018 Madurai India).
- Vinod Singh Thakur, Manikandan M, Shalini Singh, Shivam Mishra, **Ankit Kaithwas**, Mani Prabhu S S, I.A. Palani “**Laser Polishing of wire arc additive manufactured SS316L sample**” AIMTDR conference(2018)

Chapter1: Introduction.....	1
1.1 Shape memory alloy.....	1
1.2 Kapton polyimide sheet.....	2
1.3 Bimorph.....	3
1.4 Methodology.....	4
1.5 Motivation.....	4
Chapter2: Literature Review.....	7
Chapter 3: Details of Experimental Setup.....	11
3.1 Thermal evaporation system for deposition.....	11
3.2 Continuous laser for creating a pattern.....	12
3.3 Joule heating setup for investigation of actuation of the bimorph.....	13
3.4 Substrate Heating Setup for shape recovery ratio.....	14
3.5 Differential Scanning Calorimetry.....	14
Chapter 4: Result and Discussions.....	17
4.1 Patterning optimization.....	17
4.1.1 Designing of the pattern by using Kapton polyimide as a mask.	17
4.1.2 Designing of the pattern by scratching on a fully deposited film.	18
4.1.3 Designing of the pattern by using a metal grid as a mask.....	18
4.1.4 Designing of the pattern by using Kapton tape as a mask.....	19
4.1.5 Designing of the pattern by laser-fabrication.....	20

4.2	Optimization of Laser Parameter.....	21
4.3	Voltage-based Analysis with the help of Electrical Actuation on mask based pattern.....	22
(a)	<i>Circular Pattern.....</i>	22
(b)	<i>Comb-shape pattern.....</i>	23
(c)	<i>A structured Pattern.....</i>	24
(d)	<i>Deltoid Pattern.....</i>	25
(e)	<i>Fully Deposited.....</i>	27
4.4	Electrical Actuation Result of laser fabricated pattern.....	28
4.4.1	Voltage-based Analysis.....	28
(a)	<i>Circular Pattern.....</i>	28
(b)	<i>Breaded shape Pattern.....</i>	29
(c)	<i>Deltoid Pattern.....</i>	30
(d)	<i>Ladder shape Pattern.....</i>	31
(e)	<i>Comb-shape Pattern.....</i>	32
(f)	<i>Fully Deposited.....</i>	33
4.4.2	Frequency-based Analysis.....	34
(a)	<i>Circular Pattern.....</i>	34
(b)	<i>Breaded shape Pattern.....</i>	35
(c)	<i>Deltoid Pattern.....</i>	36
(d)	<i>Ladder shape Pattern.....</i>	37
(e)	<i>Comb-shape Pattern.....</i>	38
(f)	<i>Fully Deposited.....</i>	39
4.4.3	Comparison of Breaded Shape pattern and Comb-Shape Pattern	40
4.4.4	Shape recovery ratio analysis.....	45
(a)	<i>Circular Pattern.....</i>	45
(b)	<i>Ladder shape Pattern</i>	45
(c)	<i>Comb-shape Pattern</i>	46
(d)	<i>Breaded shape Pattern</i>	47

(e) <i>Fully Deposited</i>	48
4.4.5 Differential Scanning Calorimetry.....	49
4.4.6 Thickness Measurement.....	51
4.4.7 EDX.....	52
Chapter 5: Conclusion and Future scope	53
Chapter 6: References	55

LIST OF FIGURES

Fig 1:	SMA Phases and crystal structure.....	2
Fig 2:	Kapton polyimide sheet.....	3
Fig 3:	Schematic diagram of bimorph.....	3
Fig 4:	Patterned Shape Memory Alloy of thin film.....	8
Fig 5:	Displacement vs Number of cycles graph for planar fully deposited bimorph at 0.5 Hz.....	9
Fig 6:	Schematic diagram of Flash Evaporation system.....	12
Fig 7:	Ytterbium Doped Continuous Fiber Laser.....	13
Fig 8:	Schematic Diagram of Joule Heating setup.....	13
Fig 9:	Schematic Diagram of Plate Heating Setup.....	14
Fig 10:	Schematic Diagram of Differential Scanning Calorimetry.....	15
Fig 11:	Images of patterned SMA created by using Kapton polyimide as a mask.....	17
Fig 12:	Images of patterned SMA created by using the metal grid as a mask.....	19
Fig 13:	Images of patterned SMA created by using Thermal tape as a mask.....	20
Fig 14:	Images of patterned SMA created by Laser fabrication	20
Fig 15:	Voltage based Displacement vs Time graph of circular pattern.....	23
Fig 16:	Voltage based Displacement vs Time graph of comb-shape	24

	pattern.....	
Fig 17:	Voltage based Displacement vs Time graph of A structured pattern.....	25
Fig 18:	Voltage based Displacement vs Time graph of Deltoid pattern.....	26
Fig 19:	Voltage based Displacement vs Time graph of planar Fully deposited.....	27
Fig 20:	SEM images of circular pattern and Voltage based Displacement vs Time graph of circular pattern.....	29
Fig 21:	SEM images of Breaded pattern and Voltage based Displacement vs Time graph of Breaded shape pattern.....	30
Fig 22:	SEM images of Deltoid pattern and Voltage based Displacement vs Time graph of Deltoid pattern.....	31
Fig 23:	SEM images of Ladder shape pattern and Voltage based Displacement vs Time graph of Ladder shape pattern.....	32
Fig 24:	SEM images of Comb-Shape pattern and Voltage based Displacement vs Time graph of Comb-Shape pattern.....	33
Fig 25:	SEM images of Planar Fully Deposited SMA and Voltage based Displacement vs Time graph of Planar Fully Deposited.....	34
Fig 26:	SEM images of Circular pattern and Frequency based Displacement vs Time graph of Circular pattern.....	35
Fig 27:	SEM images of Breaded pattern and Frequency based Displacement vs Time graph of Breaded shape pattern.....	36
Fig 28:	SEM images of Deltoid pattern and Frequency based Displacement vs Time graph of Deltoid pattern.....	37
Fig 29:	SEM images of Ladder shape pattern and Frequency based Displacement vs Time graph of ladder shape pattern.....	38
Fig 30:	SEM images of Comb-shaped pattern and Frequency based Displacement vs Time graph of comb-shape pattern.....	39

Fig 31:	SEM images of Planar Fully Deposited SMA and frequency based Displacement vs Time graph of Planar Fully Deposited SMA.....	40
Fig 32:	Displacement vs Time graph of Comparison of Comb-shape pattern and breaded shape pattern.....	41
Fig 33:	Displacement vs Time graph of planar Fully Deposited SMA and Patterned SMA.....	42
Fig 34:	Images of Plate Heating Setup for measuring Shape Recovery Ratio.....	44
Fig 35:	Temperature vs Shape Recovery Ratio graph of Circular pattern.....	45
Fig 36:	Temperature vs Shape Recovery Ratio graph of Ladder shape pattern.....	46
Fig 37:	Temperature vs Shape Recovery Ratio graph of Comb-Shaped Pattern.....	47
Fig 38:	Temperature vs Shape Recovery Ratio graph Breaded shape pattern	48
Fig 39:	Temperature vs Shape Recovery Ratio graph of Planar Fully Deposited.....	49
Fig 40:	Temperature vs Heat flow graph of CuAlNi.....	50
Fig 41:	Measurement of thickness of CuAlNi Bimorph.....	51

List of Table

Table 1:	Aspect ratio of patterned SMA.....	7
Table 2:	Parameters of Flash Evaporation System.....	11
Table 3:	Parameter used for laser fabrication.....	21
Table 4:	Comparison of patterned SMA with Planar Fully Deposited SMA.....	42
Table 5:	Phase Transformation of CuAlNi.....	50
Table 6:	Composition analysis results obtained from EDX analysis.....	52

NOMENCLATURE

A_s Austenite start temperature

A_f Austenite finish temperature

M_s Martensite start temperature

M_f Martensite finish temperature

D_{recovery} Shape recovery ratio

ACRONYM

SMA	Shape memory alloy
SME	Shape memory effect
LDS	laser displacement sensor
SEM	Scanning Electron Microscopy
DSC	Differential scanning calorimeter
XRD	X-Ray Diffraction
OWSME	One way Shape memory effect
TWSME	Two-way shape memory effect
PE	Pseudoplastic effect
EDX	Energy dispersive X-ray Spectroscopy
PVD	Physical Vapor Deposition

Chapter 1

Introduction

1.1 Shape memory alloy

Shape memory alloy is a metal alloy capable of returning on heating to its initial shape. Even under applied load circumstances, it can recover its shape by raising the temperature, leading to high energy densities. On the application of mechanical cyclic loading, it can absorb and dissipate mechanical energy by undergoing a reversible hysteretic change. These characteristics of SMAs have made them popular for sensing and actuation, impact absorption and vibration damping applications.[1] further, these alloys have been commonly used in micro-actuators, micro-cantilevers, and micro-grippers.[2][3][4] [5]

SMA is basically categorized into two major parts on the basis of macroscopic point of view: the shape memory effect (SME), in which a specimen exhibits a large residual (apparently plastic) strain after loading and unloading that can be fully recovered upon raising the temperature of the material; and the pseudoelastic effect(PE), in which a specimen achieves a very large (apparently plastic) strain upon loading that is then fully recovered in a hysteresis loop upon unloading[4]. Practically, SMAs can exist in two different phases with three different crystal structures (i.e. twinned martensite, detwinned martensite, and austenite) and six possible transformations. The austenite structure is stable at high temperature, and the martensite structure is stable at lower temperatures[6]. When an SMA is heated, it starts to convert into the austenite stage from martensite. The Austenite temperature(A_s) is the temperature at which it is completed. Once SMA is heated beyond A_s , it starts contracting and transforming into

austenite structure, i.e. recovering into its initial shape. The conversion is feasible even under elevated loads, resulting in elevated power densities. The conversion begins to return to martensite at a martensite start temperature (M_s) during the cooling phase and it complete when it reaches the martensite Finishing temperature (M_f).

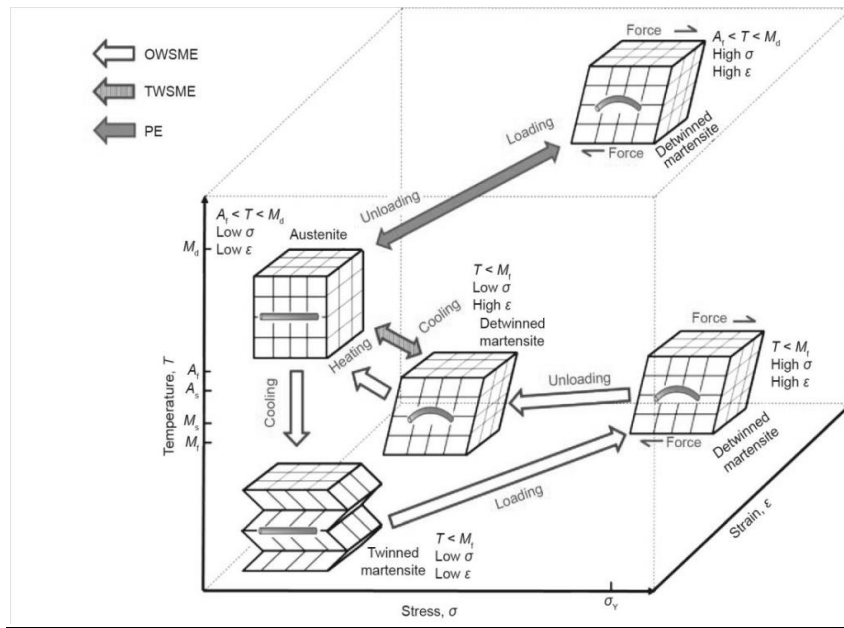


Fig.1: SMA Phases and crystal structure[7][8][9]

1.2 Kapton polyimide sheet

Kapton polyimide sheet is a hard, aromatic polyimide sheet that displays an excellent balance of electrical, chemical and physical properties over a wide range of temperature. The Kapton polyimide substrate was used for a deposition because it can withstand temperatures from $-452\text{ }^\circ\text{F}$ ($-269\text{ }^\circ\text{C}$) to $752\text{ }^\circ\text{F}$ ($400\text{ }^\circ\text{C}$). Due to this outstanding property of Kapton polyimide, it can be used at both high temperature and low-temperature extremes where other organic polymeric materials would not be

functional. The thermal conductivity of Kapton polyimide was found to be $5.24 \times 10^{-3} T^{1.02} \text{ W m}^{-1} \text{ K}^{-1}$ which helps it to actuate during actuation.[10]

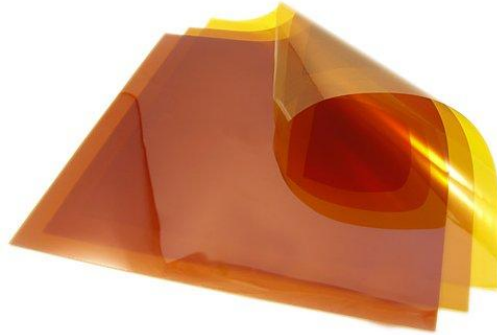


Fig.2: Kapton polyimide sheet[32]

1.3 Bimorph

Bimorph is a multilayer deposited structure which acts as a cantilever and can be used for sensing and actuation. Fig.2 shows the schematic of bimorph in which a thin film of CuAlNi is deposited over Kapton polyimide sheets. This composite layer of Kapton polyimide and a thin film of CuAlNi act as a Shape Memory Alloy.[11] Bimorphs work on a two-way effect i.e. it can remember its two different shapes. In this Bimorph one layer makes it easier to actuate during heating while others act during cooling. The deposited layer of SMA helps the bimorph to actuate during heating and Kapton polyimide sheets help it to actuate on cooling.



Fig.3: Schematic diagram of the bimorph

1.4 Methodology

A shape memory alloy is an alloy that can be deformed when cold but when heated return to its pre-deformed shape. Patterned shape memory alloy was prepared by using a ytterbium-doped fiber laser. Kapton polyimide sheet of 75 μm cut into a dimension of 3cm \times 3cm then after cleaning and baking it was clamped on the substrate holder by using thermal tape with a proper prestraining and a copper, aluminum, and nickel wires were exactly measured using a accuracy equilibrium and made into 1 gm with Cu 84.5% Ni 4% Al 12.5% by weight with 99.9% purity kept in a tungsten boat during deposition then with the help of thermal evaporation method,[12]CuAlNi was deposited over it in a high vacuum.[13] This deposition of a thin film of CuAlNi over Kapton polyimide termed as a Bimorph. This bimorph then acts as a Shape memory alloy. Bimorphs works on a two-way effect i.e. it can remember two different shapes. In this Bimorph one layer making it easier to actuate during heating while others in cooling. Thickness of thin film in a bimorph plays an important role during actuation,i.e. if the thickness of the film is very low then it restrict the bimorph to actuate, on the other hand if the thickness of the thin film is very high, then it reduces the actuation or displacement.[14]ThenUsing ytterbium-doped fiber laser,[15] the pattern was developed over the bimorph and the actuation or displacement was evaluated by the use of joule heating.[16]

1.5 Motivation

In earlier work of depositing a thin film of shape memory alloy in a planar Kapton polyimide, it was observed that during electrical actuation by means of Joule heating the flowing of current throughout the bimorph was quite smooth as a consequence it was smoothly actuated and also provides a very high displacement. It was also observed that the displacement of a

planar bimorph gets reduced on increasing the load.[5].Therefore the primary motive to create the pattern on a planar bimorph was the load reduction because of the removal of the deposited material.

Summary

In this chapter, we studied the following things which can be summarized as follows:

- Shape memory alloy is a metal alloy which is capable of returning to its original shape upon heating.
- Shape memory alloy can be used in microgrippers, micro-actuators, and microcantilever.
- Kapton polyimide sheet is a hard, aromatic polyimide sheet which can be used at both high temperature and low-temperature extremes where other organic polymeric materials would not be functional.
- Bimorph is a multilayer deposited structure in which one layer making it easier to actuate during heating while others in cooling
- Patterning on a planar fully deposited film can be done by using ytterbium-doped fiber laser.
- The primary motive to create the pattern on a planar bimorph was the load reduction because of the removal of the deposited material.

-

Chapter 2

Literature Review

This chapter gives an insight into the past work done on the Kapton polyimide substrate. It also shows the analysis done on the deposited material over the Kapton polyimide substrate and the effect of patterning over the Kapton polyimide substrate.

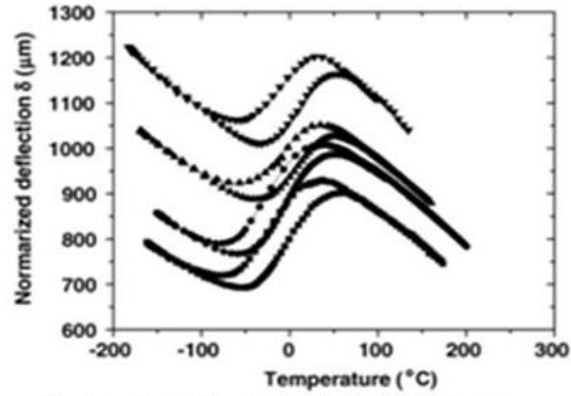
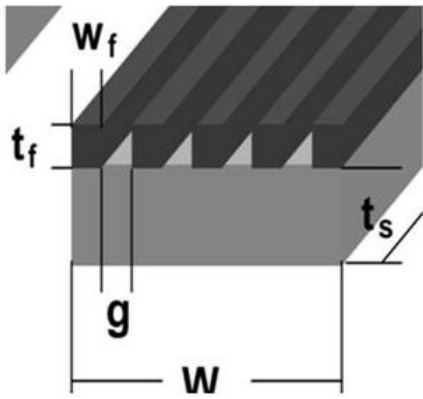
Kiyotaka Mori[17] did the experimental study on the patterned shape memory alloy thin film to find out the actuation of patterned shape memory alloy films in comparison to the planar shape memory alloy thin films and observed that the uniaxial stress field in shape memory alloy(SMA) films patterned into thin films improves SMA/Si cantilever bimorphs transformation induced deflection compared to planar film cantilevers, and also observe that In the single-phase temperature ranges $T > A_f$, M_s and $T < A_s$, M_f (A_f -austenite finish, A_s -austenite start, M_f -martensite finish and M_s -martensite start temperatures), where the deflection is controlled by the thermoelastic stress, the change reflects the difference between the uniaxial and biaxial stress states.

Sample no.	Aspect ratio t_f / w_f
1	0.31
2	0.16
3	0.016
4	0.0009

t_f = thickness of deposition

w_f = width of deposition

Table 1: Aspect ratio of patterned SMA



kiyotaka mori Jian Li Alexander L Roytburd and Manfred wutting

Deflection of four differently patterned NiTi/Si bimorph cantilevers as a function of temperature. All bimorphs were processed simultaneously and identically.

- ■ ■ (full squares)-sample 1 aspect ratio = 0.31,
- ● ● (full circles)-sample 2 aspect ratio = 0.16,
- ▲ ▲ ▲ (tip up full triangles)-sample 3 aspect ratio = 0.016,
- ▼ ▼ ▼ (tip down full triangles)-sample 4 aspect ratio = 0.0009

Fig.4: Patterned Shape Memory Alloy of thin film

The data in Fig.(4) show that the deflection of the NiTi/Si composite cantilever depends on the aspect ratio t_s/w in the high, $T > A_f$ or M_s (austenite phase), intermediate $A_s < T < A_f$ or $M_f < T < M_s$ (austenite plus martensite phases), and low, $T < A_s$ or M_f (martensite phase), temperature regimes. Quantitatively, the deflection is measured by the slope $d\delta/dT$.

K AKASH did the experimental study on the planar thin film of shape memory alloy in which he examined the displacement of shape memory alloy at different voltage and different frequency and observed that the maximum displacement obtained by a planar CuAlNi bimorph was approx. 1.6 mm at 0.5 Hz. Fig. (5) depicted the time vs displacement graph of a planar shape memory alloy bimorph.

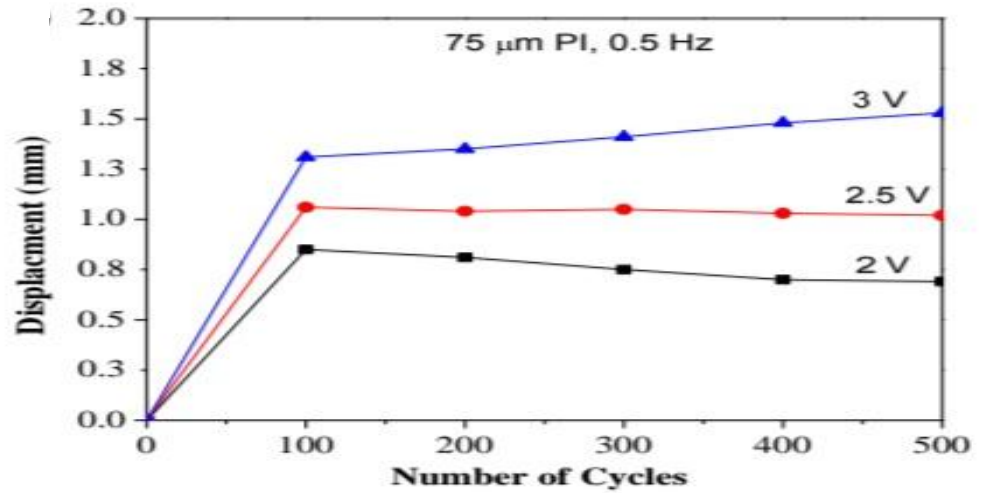


Fig 5: Displacement vs Number of cycles graph for planar fully deposited bimorph at 0.5 Hz.[14]

Summary

This chapter gives an insight into the past work done on the Kapton polyimide substrate which can be summarized as follows:

- The uniaxial stress field in shape memory alloy(SMA) films patterned into thin films improves SMA/Si cantilever bimorphs transformation –induced deflection compared to planar film cantilevers.
- The maximum displacement obtained by a planar CuAlNi bimorph was approx. 1.6 mm at 0.5 Hz.

CHAPTER 3

Details of Experiment

3.1 Thermal evaporation system for deposition

Thermal evaporation method has used for deposition of CuAlNi over the Kapton polyimide sheets of thickness 75 μ m. It works on the principle of the physical vapor deposition process. [18]Physical vapor deposition (PVD) describes a variety of vacuum deposition methods which can be used to produce thin films and coatings. PVD is characterized by a process in which the material goes from a condensed phase to a vapor phase and then back to a thin film condensed phase. Tungsten boat was used for placing SMA wires in a high vacuum chamber and a prestrained Kapton polyimide sheet was clamped on the substrate holder. The polyimide sheets were baked and cleaned before the deposition. During a deposition, this SMA wire gets melted, evaporated and then deposited on a Kapton polyimide substrate.

Parameters	value
Substrate	Kapton polyimide substrate
Thickness of substrate	75 μ m
Distance between wire holder and substrate	150mm
Composition of material	Cu 84.5 wt%, Ni 4 wt%,Al 11.5 wt%
Current	350 A
Wire holder	Tungsten crucible
Vacuum	0.05 mbar

Table 2: Parameters of Flash Evaporation System

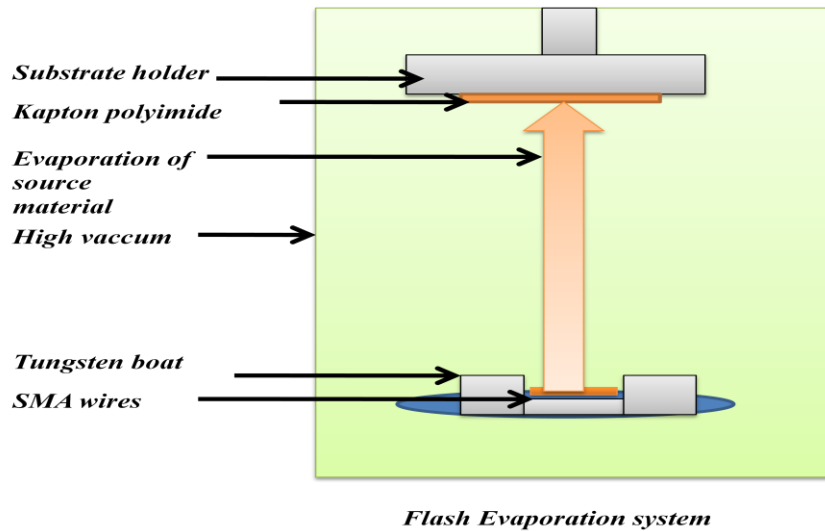


Fig. 6: Schematic diagram of Flash Evaporation system

3.2 Continuous laser for creating a pattern

Laser is a device that stimulates atoms or molecules to emit light at particular wavelengths and amplifies that light, typically producing a very narrow beam of radiation. Continuous laser is a kind of laser in which the laser is continuously pumped and continuously emits light. Ytterbium (Yb) doped continuous fiber laser machine is used as a source of power for the removal of deposited material from Kapton polyimide substrate for creating a pattern. The wavelength of the laser used was 1064 nm and the focal length as of 300mm. With the help of optimization of parameters of the laser, deposited material can easily be removed from the bimorph.

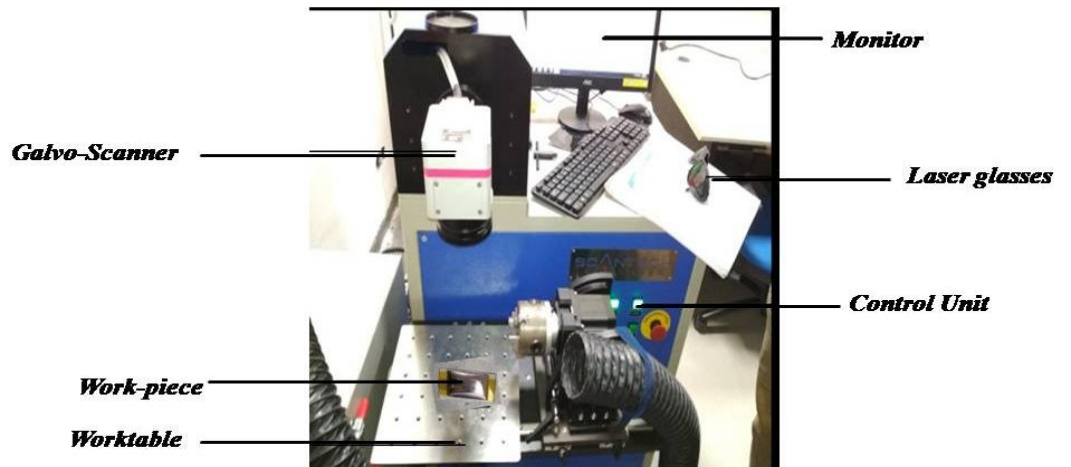


Fig 7: Ytterbium Doped Continuous Fiber Laser

3.3 Joule heating setup for investigation of actuation of the bimorph

A thermo-mechanical setup using Joule heating was utilized to find out the actuation behavior of bimorph. Various properties of actuation such as frequency, current, voltage varied to observed the maximum displacement for different patterned bimorph. Fig.(8) shows the schematic diagram of joule heating setup. In that bimorph was clamped as a cantilever in a bimorph holder and displacement can be measured with the aid of laser displacement sensor.

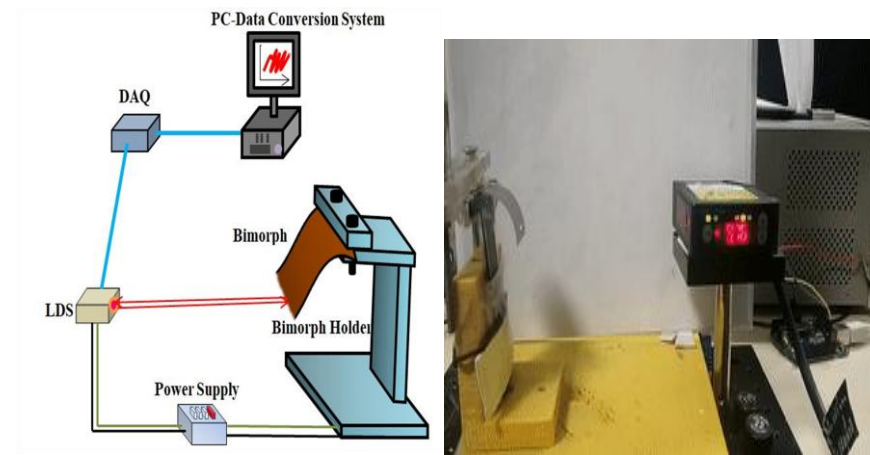


Fig 8: Schematic Diagram of Joule Heating setup

3.4 Substrate Heating Setup for shape recovery ratio

Plate heating setup was utilized to find out the shape recovery ratio of a bimorph. Shape recovery ratio was measured by calculating the inner and outer diameter of bimorph at a distinct temperature. To investigate the shape recovery ratio bimorph of 3cm×2cm clamped like a butterfly structure which can be shown in Fig.(9) with Kapton tape or thermal tape at the center of a substrate heater and then calculated the value of its inner and outer diameter at a distinct temperature.



Fig 9: Schematic Diagram of Plate Heating Setup

3.5 Differential scanning calorimetry

Differential Scanning Calorimetry or DSC is a thermoanalytical method in which the difference in the quantity of heat needed to raise a sample's temperature and reference is measured as a function of temperature. Throughout the experiment, the sample and reference are retained at almost the same temperature. The temperature program for a DSC analysis is generally designed to increase the temperature of the sample holder linearly as a function of time. The reference sample should have a well-defined heat capacity over the Scanning spectrum of temperatures.[19]

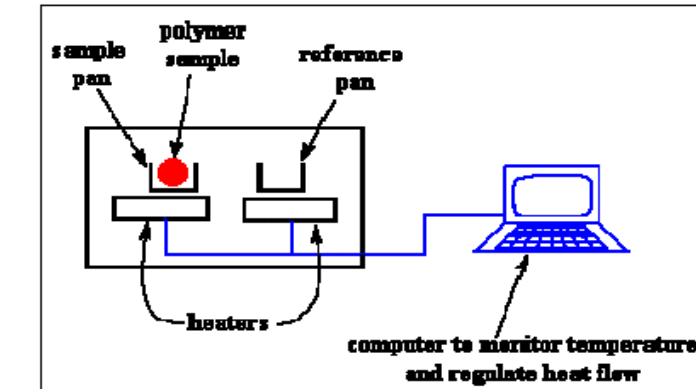


Fig 10: Schematic Diagram of Differential Scanning Calorimetry

Summary:

This chapter deals with the Experimental setup used during the complete procedure which can be summarized as follows:

- PVD is a process in which the material goes from a condensed phase to a vapor phase and then back to a thin film condensed phase. This method was used for the deposition of CuAlNi over Kapton polyimide.
- Continuous laser is a kind of laser in which the laser is continuously pumped and continuously emits light. Ytterbium-doped fiber laser was used for the removal of deposited material from the bimorph.
- A thermo-mechanical setup using Joule heating was utilized to find out the actuation behavior of bimorph.
- Plate heating setup was utilized to find out the shape recovery ratio of a bimorph.
- Differential Scanning Calorimetry or DSC is a thermoanalytical method in which the difference in the quantity of heat needed to raise a sample's temperature and reference is measured as a function of temperature. It was used to find out the A_s , A_f , M_s & M_f temperature.

Chapter 4

Result and Discussion

4.1 Patterning optimization

By using kapton polyimide sheet as a mask

By scratching on fully deposited thin film.

By using metal grid as a mask

By using kapton tape as a mask.

By using laser fabrication.

4.1.1 Designing of the pattern by using Kapton polyimide as a mask

Designing the pattern is followed by a number of distinct methods. For creating patterns over thin film deposition, a Kapton polyimide sheet used as a mask .For this, a mask of Kapton polyimide sheet added over the Kapton polyimide substrate with the help of Kapton tape. But due to the improper contact of one Kapton polyimide sheet over another one, the material gets deposited in the unwanted surface as depicted in Fig.(16), as a result of which undesirable pattern was obtained.



Fig 11: Images of patterned SMA created by using Kapton polyimide as a

Mask

4.1.2 Designing of patterns by scratching on a fully deposited thin film

Patterning on fully deposited bimorph is also tried by scratching on a fully deposited bimorph, for this Initially SMA deposited over Kapton polyimide sheets, then scratching tried over it with sharp material for creating a pattern as a result of which surface of bimorph get deteriorated and the dimensions of structure in fully deposited also gets affected. Due to this reason, it shows negligible actuation in joule heating because of the improper path of flowing current in a bimorph.

4.1.3 Designing of pattern by using the metal grid as a mask

Designing of Rhombus like structure was tried by using the metal grid as a mask during deposition. For this metal grid attached over the Kapton polyimide sheets before deposition. Fig. (12a) shows the attachment of a metal grid over the Kapton polyimide sheet. Fig. (12b) shows the rhombus patterned structure(i.e. the final pattern obtained after deposition). But the limitation of using the metal grid for a mask is only one i.e. rhombus shape patterned can be obtained. The main drawback of using the metal grid for the pattern was the flow of current, due to the gap between the two structured part current was not getting the proper way to flow throughout the structure result of which SMA bimorph loses its actuation characteristics.

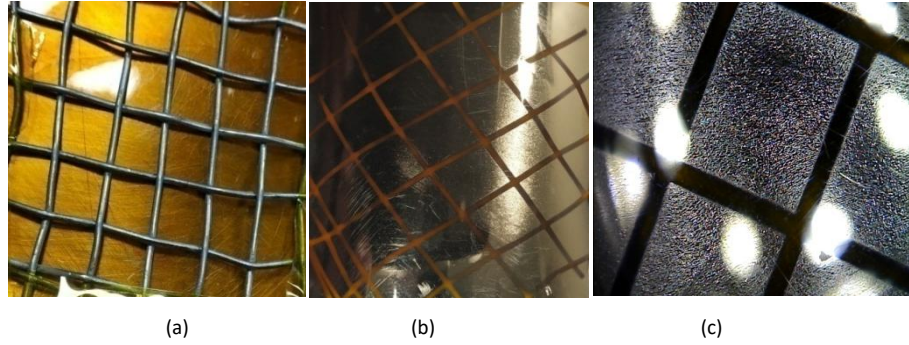


Fig. 12: Images of patterned SMA created by using metal grid as a mask

4.1.4 Designing the pattern by using Kapton tape as a mask

Designing of pattern over Kapton polyimide sheet by using Kapton tape as a mask. For creating a pattern in a bimorph, Kapton tape was used to stick it over the Kapton polyimide sheet before deposition. Fig. (13a) shows the shape before deposition, On completion of deposition Kapton tape which acts as a mask during deposition was removed to get the final shape. Fig. (13b) shows the actual shape or final patterned structure of bimorph after deposition. The main advantage of using Kapton tape as a mask that receiving the number of distinct shapes by using a Kapton tape in an appropriate manner, but the main drawbacks of using Kapton tape as a mask was dimensions of patterned structure gets affected on removal of Kapton tape after deposition because on removing the Kapton tape from Kapton polyimide sheets, some nearby deposited area also gets come out which directly affect the dimensions of patterns. The main limitation of Kapton tape as a mask was that it cannot be used for a small dimension.

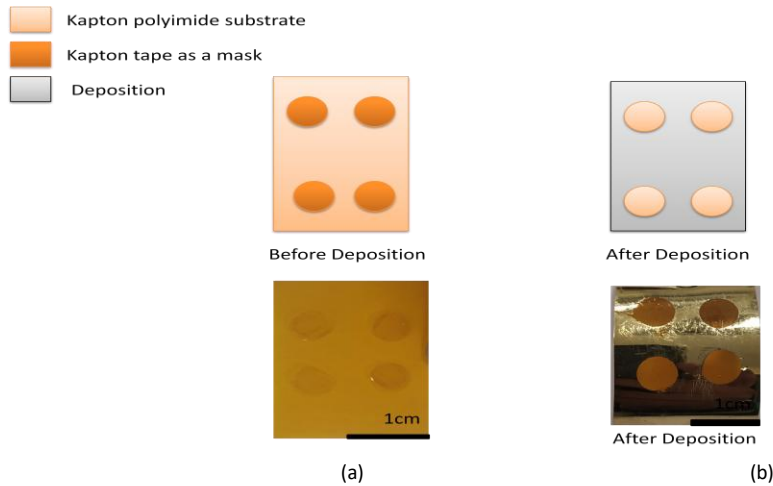


Fig. 13: Images of patterned SMA created by using Thermal tape as a mask

4.1.5 Designing of pattern by laser fabrication

Pattern designing by laser fabrication is one of the best methods among all these methods. By these method different shapes can be fabricated over the fully deposited bimorph by using laser under optimum condition.[20][21] This method helps to overcome the limitation of creating small shapes in a fully deposited bimorph and dimensions of the patterned structure were also not affected because the process of removal of the mask from bimorph gets eliminated. Fig. (14) shows the pattern created by laser fabrication.

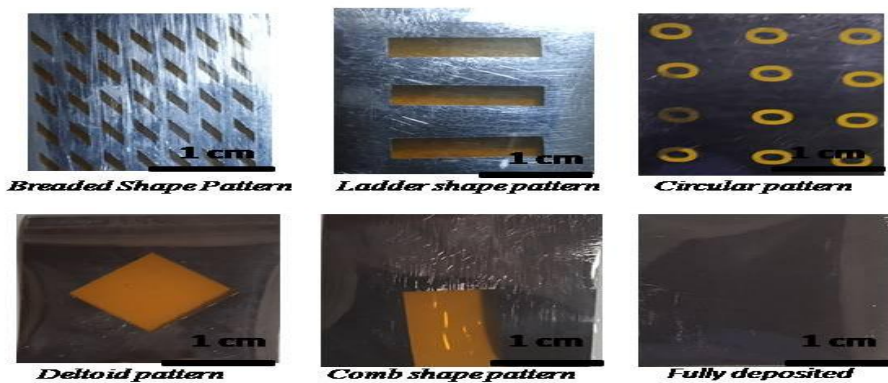


Fig. 14: Images of patterned SMA created by Laser fabrication

4.2 OPTIMIZATION OF LASER PARAMETER

Wavelength(nm)	Power(w)	No. of passes	Stand of distance(mm)	
1064	5	2	300	
1064	10	1	300	
1064	10	2	300	
1064	15	1	300	
1064	15	2	300	
1064	20	1	300	
1064	20	2	300	
1064	25	1	300	
1064	25	2	300	

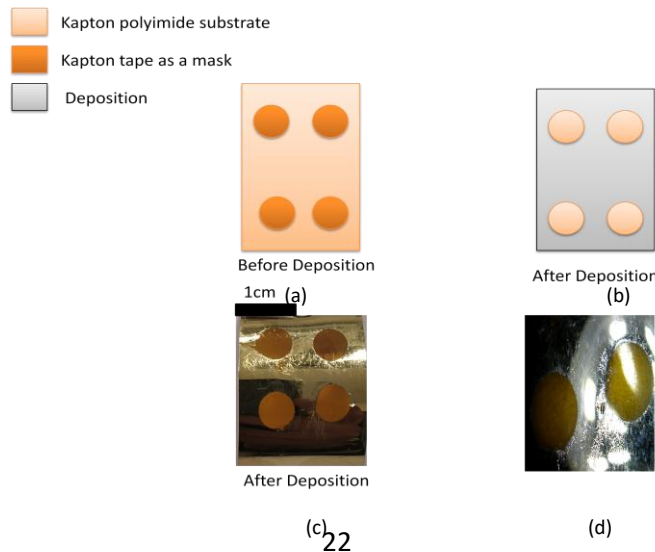
Table 3: Parameter used for laser fabrication

Table(3) shows the optimization of parameters of laser by varying power, number of passes, Stand of distance. During the experimental study, it was observed that the optimized parameter for complete removal of CuAlNi deposition from the Kapton polyimide substrate without any effect on it was 20 watt, single pass with a stand of distance(i.e. the distance between the object and the laser) of 300mm. from table(3) it can be concluded that on using 5W and double pass there was no changes in a deposited SMA which can be seen in row 1 of table 3 but on increasing the power from 5W to 10W deposited material starts removing as shown in row 3 and at 20W with a single pass, deposited SMA was completely removed from Kapton polyimide sheet as shown in row 5, and on further increasing the power from 20W to 25W deposited material starts burning, which can be depicted in table 3 row 9.

4.3 VOLTAGE ANALYSIS WITH THE HELP OF ELECTRICAL ACTUATION ON MASK BASED PATTERN

(a) Circular pattern

For designing a pattern in a deposited bimorph, a circular mask of Kapton tape was created. further, this circular mask of Kapton tape was made to stick on a Kapton polyimide substrate and by means of physical deposition method[7], CuAlNi was deposited over it and on completion of deposition after the circular mask was removed from the bimorph. Fig. (15a) shows the schematic of the circular pattern before deposition and after deposition Fig. (15b) shows the actual image of a pattern after deposition and Fig (15d) shows the microscopic images of the circular pattern. To investigate the actuation and displacement of bimorph, Joule heating was used and observed a max displacement of 0.67,1.75,1.83 mm at 1V,2V, and 3V respectively. Fig (15) shows the graph of displacement of bimorph at distinct voltage.



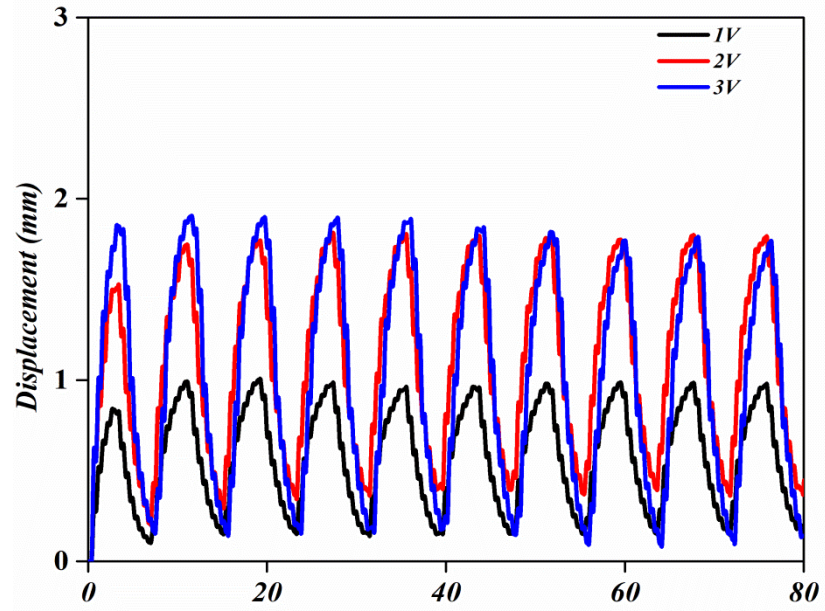


Fig. 15: Voltage based displacement vs time graph of a circular pattern

(b) Comb-Shaped pattern

The comb-shaped pattern was created by using a Kapton tape in a rectangular shape as a mask over the Kapton polyimide sheet before deposition. Once the deposition completed Kapton tape was removed from the bimorph and a final shape which is shown in Fig(16c) had framed. Fig (16a) and Fig. (16b) shows the schematic diagram of the comb-shaped pattern before deposition and after deposition. Max displacement obtained in a comb-shaped pattern was 0.56, 3.08, 3.12 at 1V, 2V, and 3V respectively. Fig. (16) shows the graph of displacement at a distinct voltage.

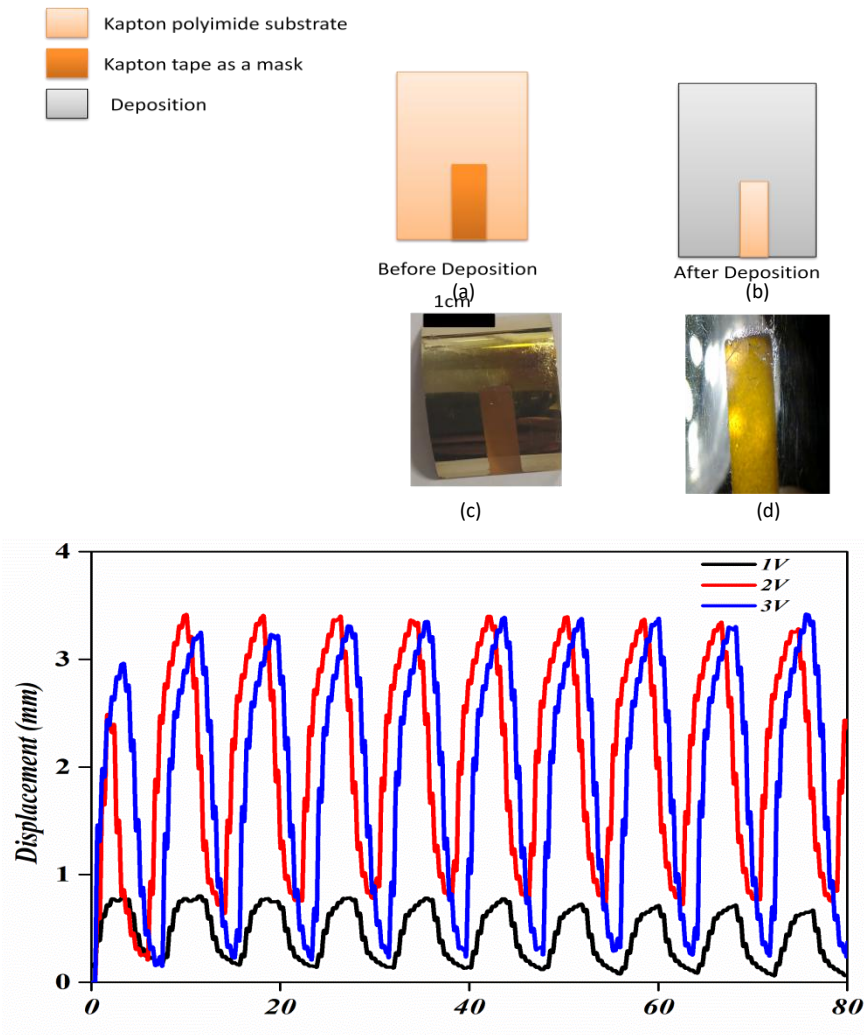


Fig. 16: Voltage based displacement vs time graph of the comb-shaped pattern.

(c) A Structured Pattern

A rectangular Kapton tape was used to create a mask for making alphabetically A structured pattern. The main reason for creating for this kind of pattern was to optimize the pattern which can provide better displacement than the fully deposited pattern. Mostly the displacement or actuation depends on the path in which the current is flowing and the amount of SMA deposited. From the A structured type

pattern it was observed that the maximum displacement was 0.57,1.56,and2.13at 1V,2V,and3V respectively.

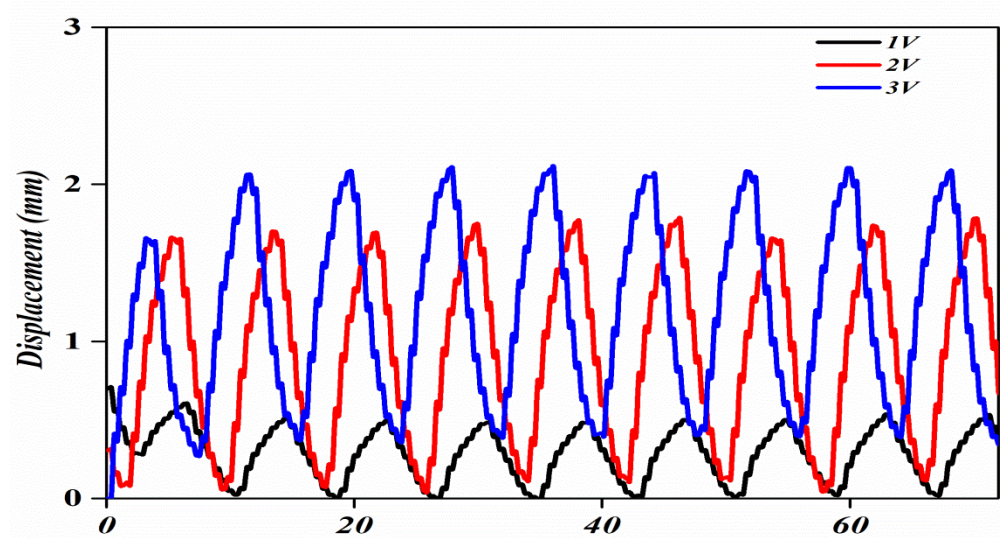
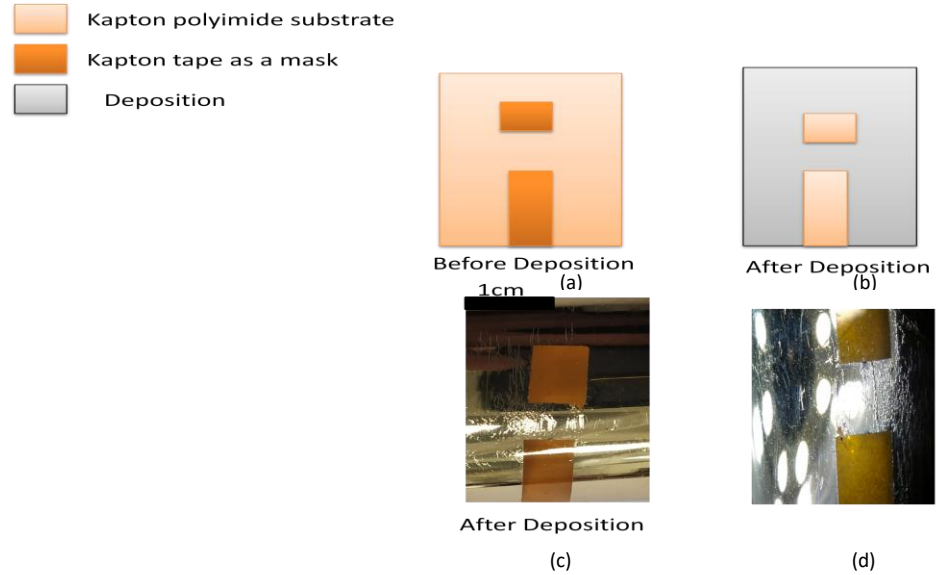


Fig. 17: Voltage based displacement vs time graph of A structured pattern

(d) Deltoid pattern

A deltoid pattern was tried to created by the rectangular mask of Kapton tape in a Kapton polyimide substrate. For this, a rectangular

mask was created by a Kapton tape and pasted it on a Kapton polyimide substrate diagonally, then after deposition that rectangular mask was removed from the bimorph and a deltoid pattern was obtained. Fig (18a)& Fig. (18b) shows the schematic diagram of the deltoid pattern before deposition and after deposition and Fig. (18d) shows the microscopic images of deltoid pattern. Fig. (18) shows the graph of displacement of deltoid pattern, 0.32, 0.67, 0.87 displacement in mm at 1V, 2V, and 3V was observed in a deltoid pattern.

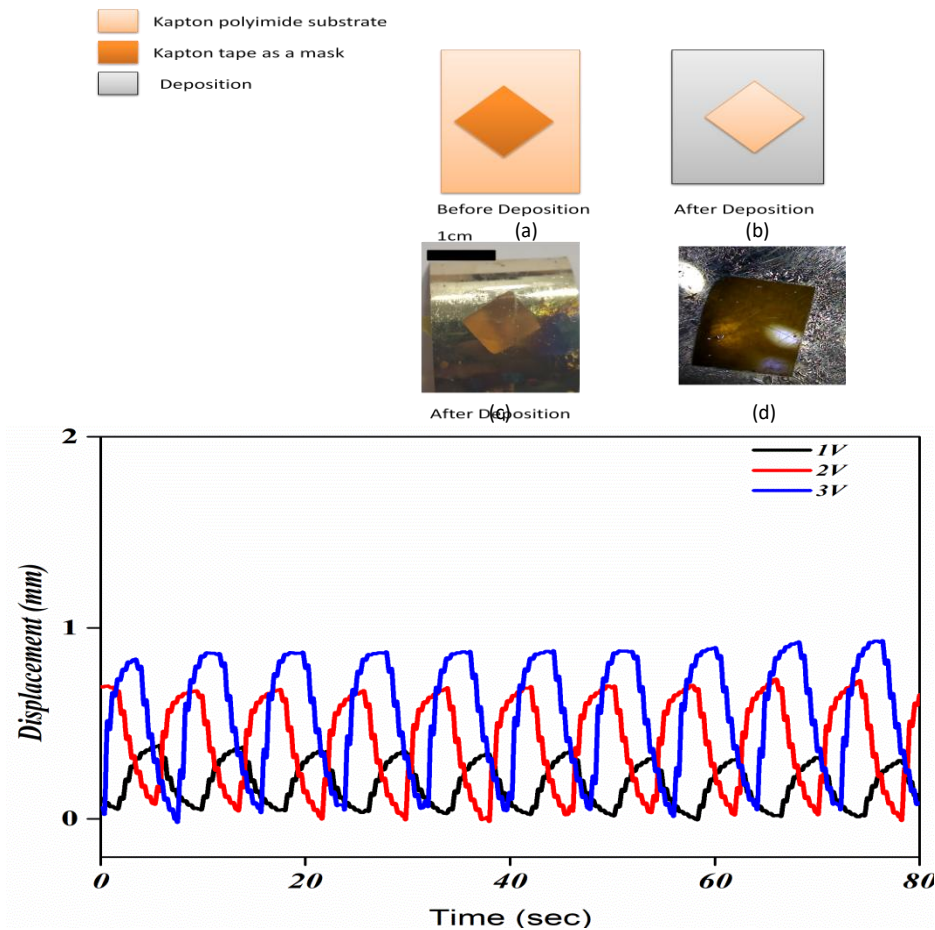


Fig. 18: Voltage based displacement vs time graph of Deltoid pattern

(e) Fully Deposited

Fig (19a)&Fig (19b) shows the schematic diagram of fully deposited SMA on a Kapton polyimide sheet and the Fig. (19d) shows the microscopic images of fully deposited bimorph. Fig. (19) shows the graph of maximum displacement at a different voltage. Maximum displacement observed was 0.54, 1.67, 3.33 at 1V, 2V and 3V respectively. [14]

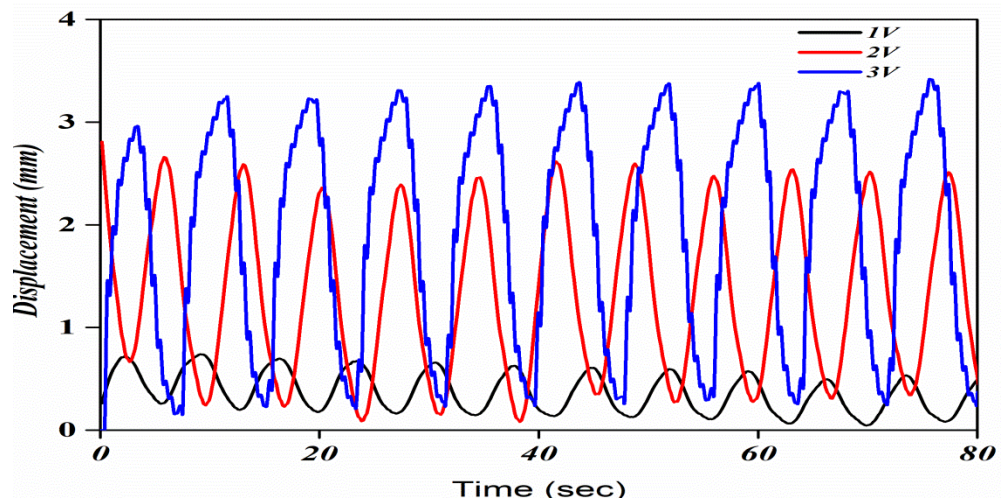
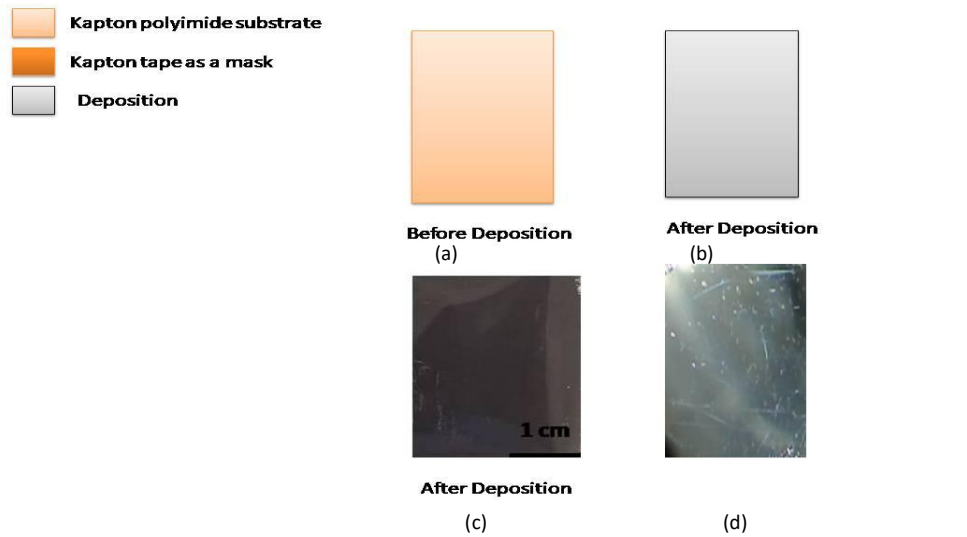


Fig. 19: Voltage based displacement vs time graph of planar Fully deposited

In the end, On comparing all the patterns with the fully deposited pattern, it was observed that none of the pattern was providing the better maximum displacement in comparison to the fully deposited pattern at a particular voltage. The main reason for not getting a good result was the flow of current. In most of the pattern, the current was not getting the proper path in a particular time so that it lost its path in somewhere between the bimorph, due to which it was not displaced properly.

4.4 Electrical actuation of laser fabricated pattern

4.4.1 Voltage-based analysis

(a) Circular pattern

To find out the maximum displacement, a number of the different pattern was created over the fully deposited thin film of SMA. Fig. (20) shows the SEM images of the circular pattern. For creating a circular pattern number of circles were created all over the surface of the thin film of $3 \times 2 \text{ cm}^2$ with the help of continuous laser. To investigate the cyclic behavior and maximum displacement of patterned bimorph, electrical actuation was tried over it with the help of Joule heating[14]. Fig (20) shows the graph of maximum displacement of the circular patterned deposited sample over Kapton polyimide sheet and it was observed that at displacement gets increased on increasing the voltage and the maximum displacement of about 2.24 was obtained at 3V, which was 1.54 and 0.64 at 2V and 1V respectively. It was also observed that the sample was getting burnt at 4V.

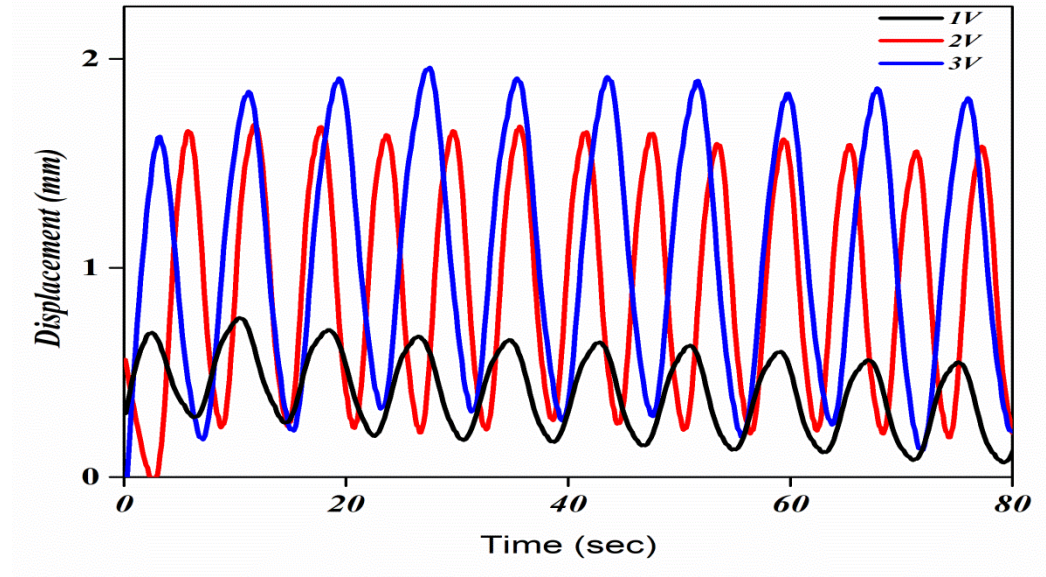
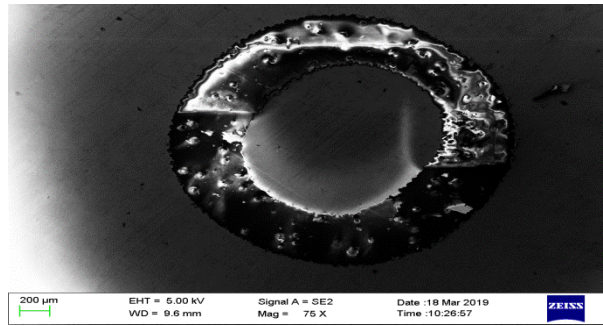


Fig. 20: SEM images of circular pattern and Voltage based displacement vs time graph of a circular pattern

(b) Breaded shape Pattern

Fig(21) shows the SEM images of Breaded pattern. For designing a breaded pattern, a number of squares diagonals were created on the surface of fully deposited SMA bimorph of $3 \times 2 \text{ cm}^2$. Fig. (21) shows the displacement of breaded patterned SMA thin films and it has observed that the displacement obtained was 0.41,1.35,1.58 in mm at 1V,2V, and 3V respectively. It was also observed that it was not getting burnt on increasing the voltage over 3V and providing displacement of about 7.57 at 4V 3A.

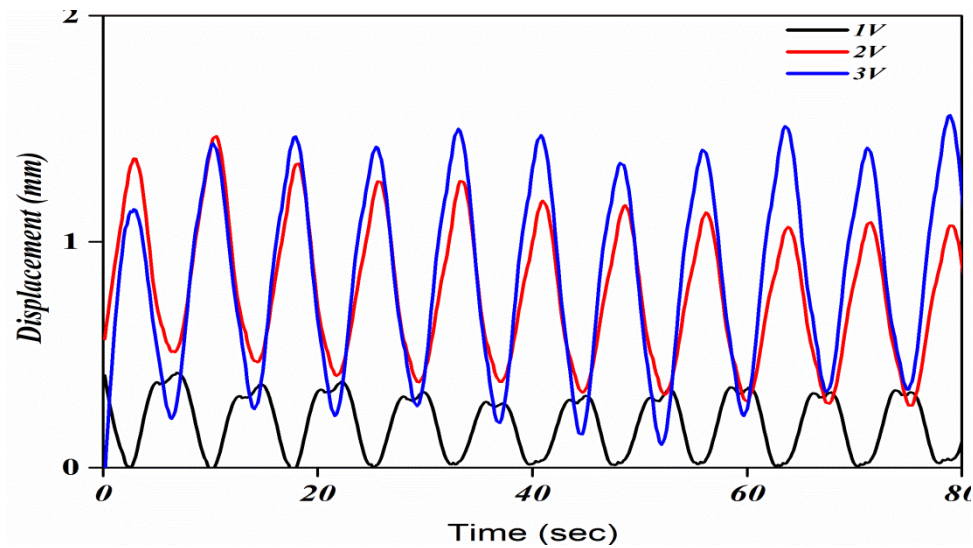
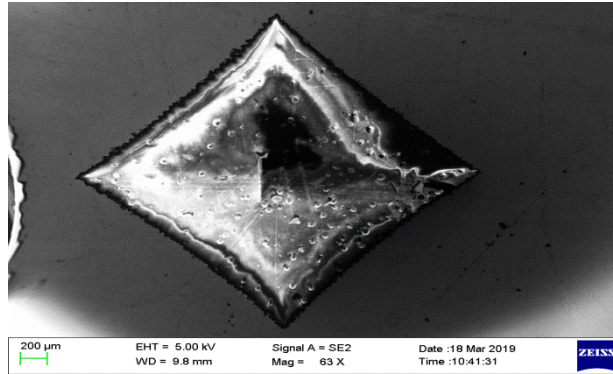


Fig. 21: SEM images of Breaded pattern and Voltage based displacement vs time graph of Breaded pattern

(c) Deltoid Pattern

Fig. (22) shows the SEM images of the Deltoid pattern. For creating a deltoid pattern a square diagonal was created on the surface of a thin film of SMA on the substrate of Kapton polyimide sheets of dimensions 3×2 cm². To investigate the maximum displacement of Deltoid pattern, electrical actuation has done with the help of joule heating and it was observed that it provides the maximum displacement among all the pattern. The max displacement achieved was 0.50, 3.43 and 4.10 at 1V, 2V, and 3V respectively. Fig. (22) shows the graph of max displacement at 1V, 2V, and 3V.

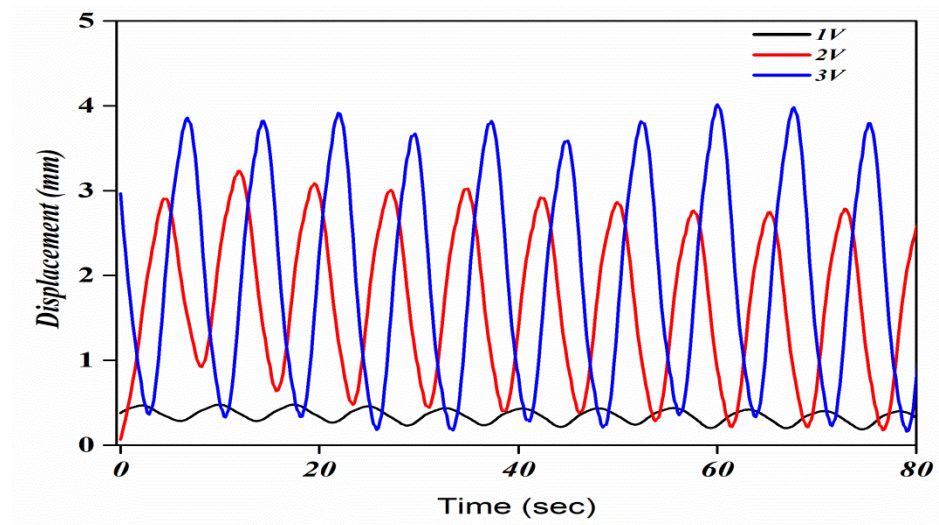
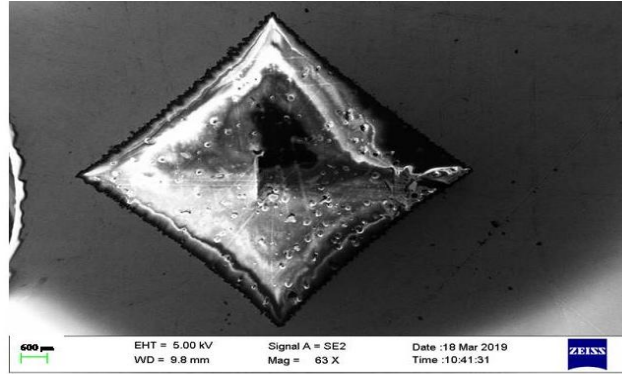


Fig. 22: SEM images of Deltoid pattern and Voltage based displacement vs time graph of Deltoid pattern.

(d) Ladder shape pattern

Designing of ladder pattern has been done by removal of 4 rectangular shapes of dimension, 3mm×10mm from fully deposited SMA over Kapton polyimide sheets of dimension 30mm×20mm with the help of continuous layer. Fig. (23) shows the SEM images of ladder patterned structure. With the help of electrical actuation, displacement of 0.44, 1.20, 1.29 was observed at 1V, 2V, and 3V respectively. Fig. (23) shows the graph of actual displacement of ladder patterned SMA bimorph at 1V 2V and 3V.

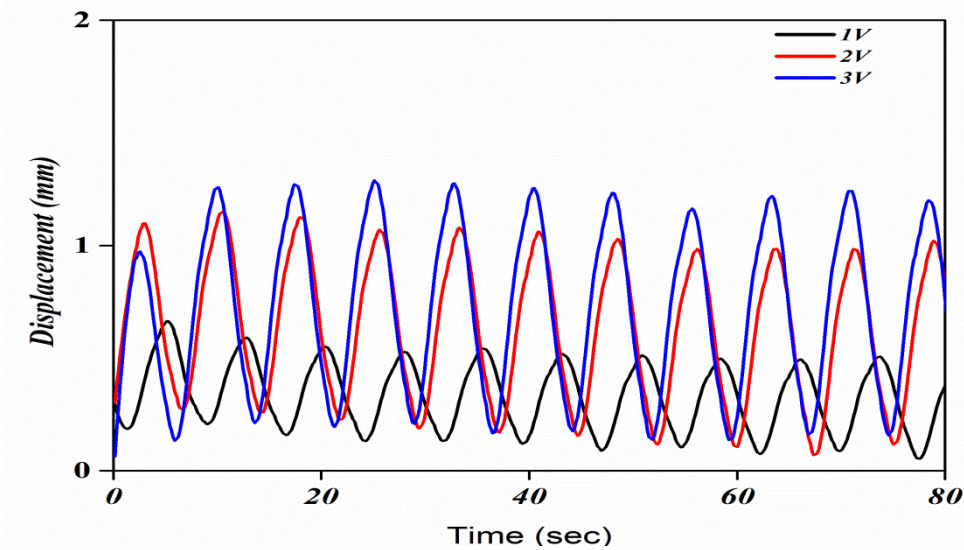
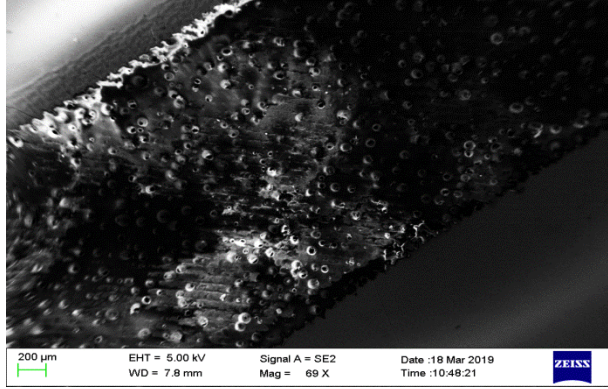


Fig. 23: SEM images of Ladder pattern and Voltage based displacement vs time graph of Ladder pattern

(e) Comb-Shape pattern

Designing of the comb-shaped pattern has done by removal of the rectangular shape of the dimension of 15mm×8mm from a fully deposited SMA thin film of dimension 30mm×20mm. Fig. (24) shows the SEM image of the comb-shaped pattern structure. The maximum displacement of 0.48,2.34,3.52 was observed at 1V,2V, and 3V respectively.Fig (24)shows the graph of maximum displacement at a different voltage. It gives the maximum displacement of 8.02 at 4V and 3A.

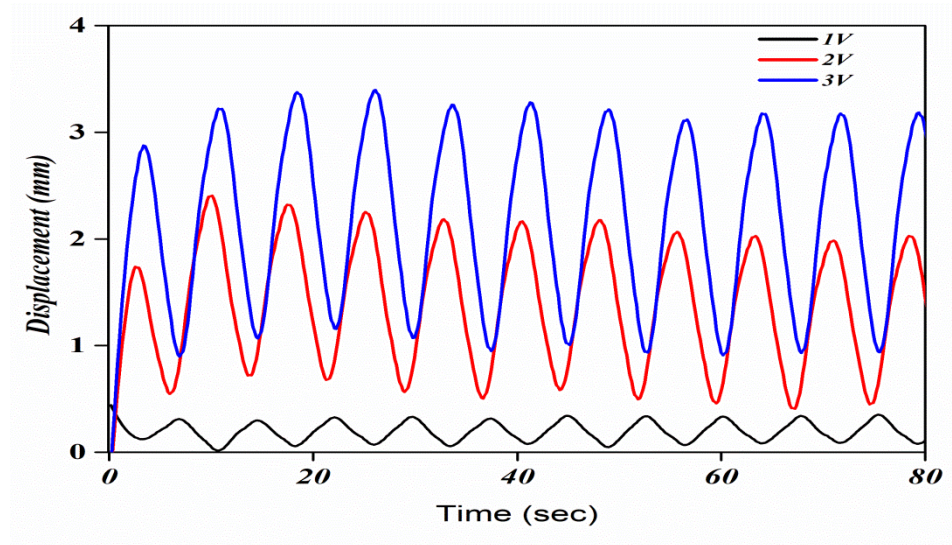
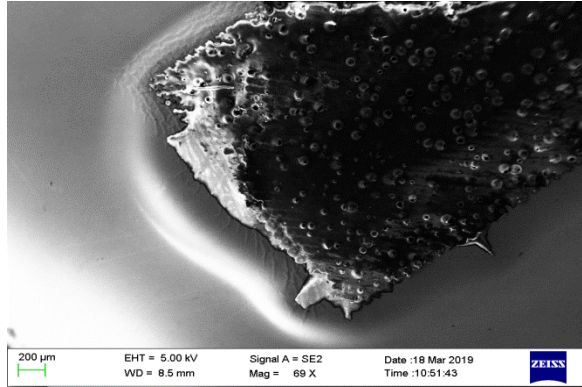


Fig. 24: SEM images of Comb-Shaped pattern and Voltage based displacement vs time graph of Comb-Shaped pattern

(f) Fully Deposited

Fig. (25) shows the SEM images of fully deposited SMA of CuAlNi thin film over Kapton polyimide substrate of dimension 30mm×20mm. Fig. (25) shows the graph of maximum displacement at a different voltage. Maximum displacement observed was 0.54, 1.67, 3.33 at 1V, 2V and 3V respectively.

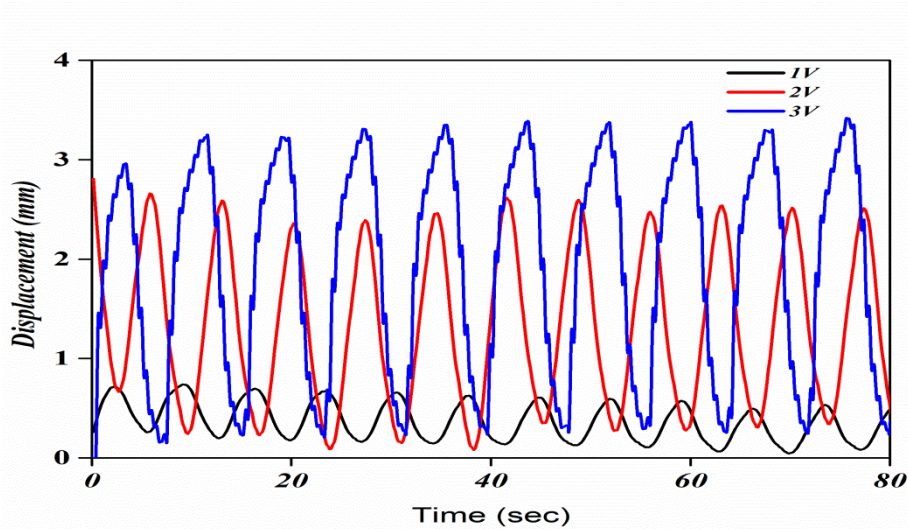
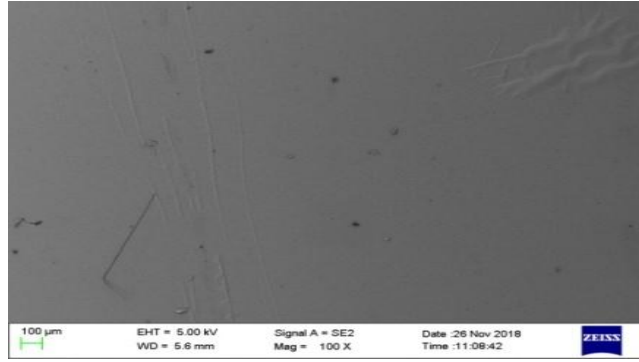


Fig. 25: SEM images of Planar Fully Deposited SMA and Voltage based displacement vs time graph of Planar Fully Deposited SMA.

4.4.2 Frequency-based analysis

(a) Circular pattern

Investigation of maximum displacement has done on the basis of frequency, It was observed that the maximum displacement of the circular pattern was 0.90,1.82,2.18 at 0.50,0.33 and 0.25Hz respectively. Fig. (26) shows the graph of actual displacement of the circular pattern at three different frequency, it was also observed that on increasing the frequency more than 0.50 it shows a negligible displacement and it shows almost same displacement on decreasing the frequency.

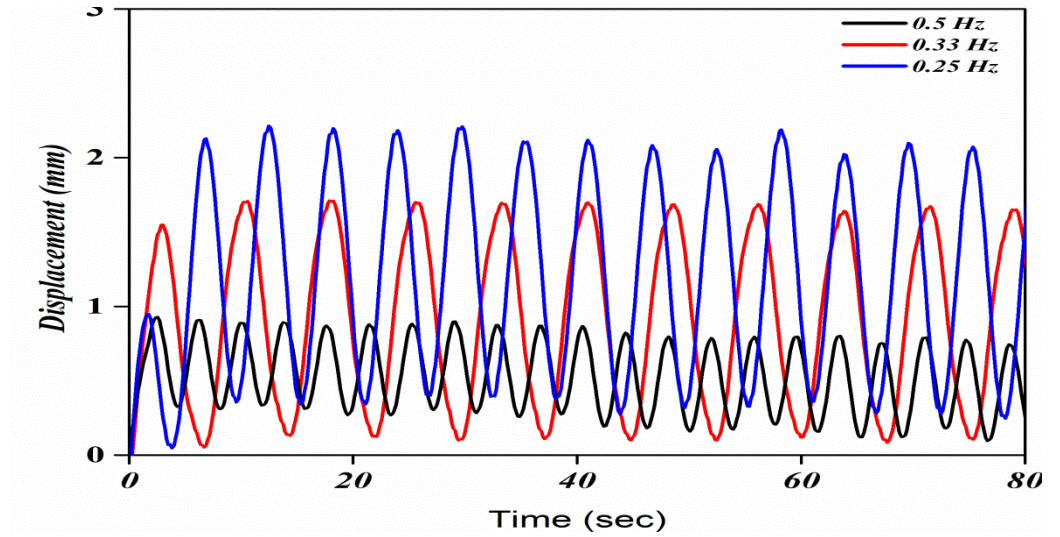
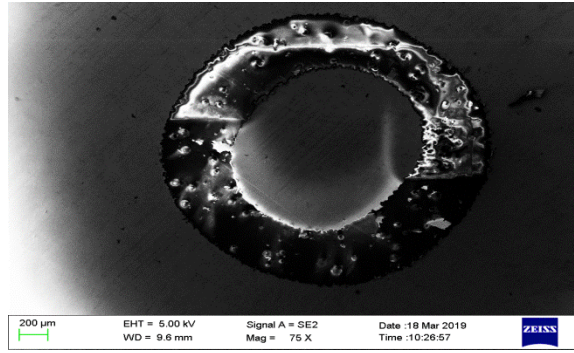


Fig. 26: SEM images of Circular pattern and Frequency based displacement vs time graph of Circular pattern.

(b) Breaded shaped pattern

In a breaded shaped pattern, it was found that the maximum displacement obtained was 0.94, 1.34 and 1.58 in mm at 0.5, 0.33 and 0.25 Hz respectively whose Displacement vs Time graph can be displayed as shown in Fig. (27)

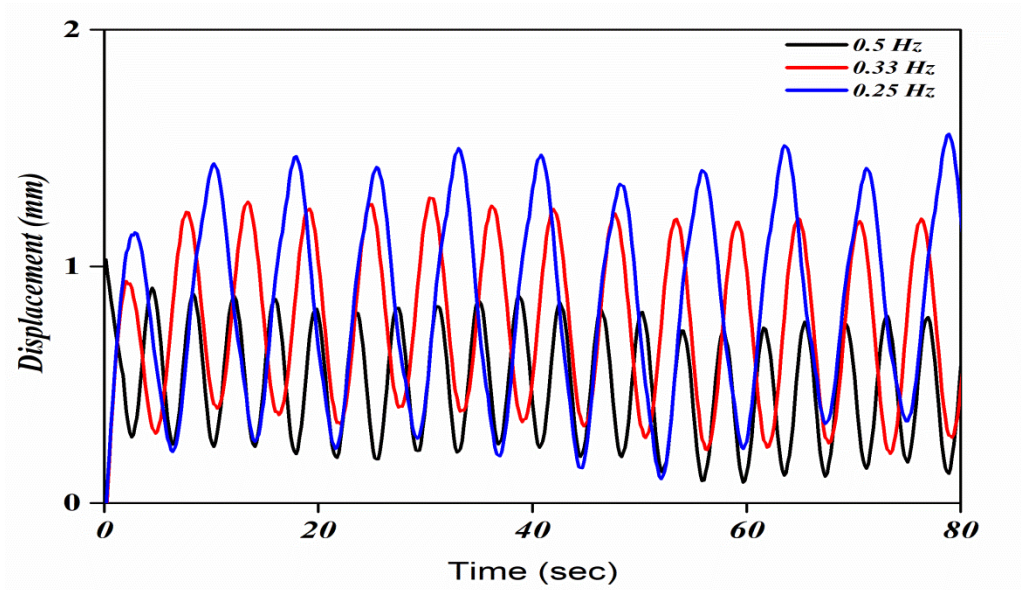
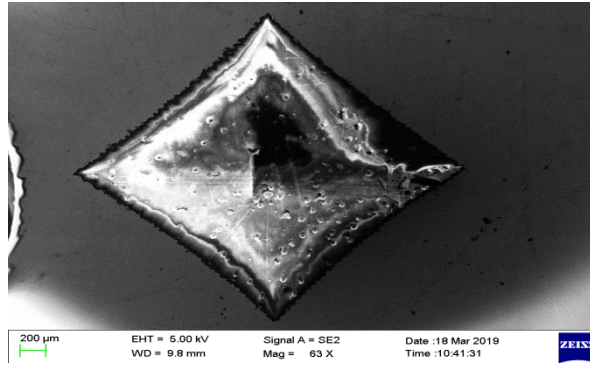


Fig. 27: SEM images of Braided pattern and Frequency based displacement vs time graph of Braided pattern.

(c) Deltoid Pattern

Fig. (28) shows the SEM images of the deltoid pattern. Maximum displacement investigation was conducted on the basis of frequency for the Deltoid pattern and it has been observed that the maximum displacement was 2.38, 3.38 and 4.18 in mm at 0.50Hz, 0.33Hz, and 0.25Hz respectively which can be shown by Displacement vs Time graph as shown in fig(28).

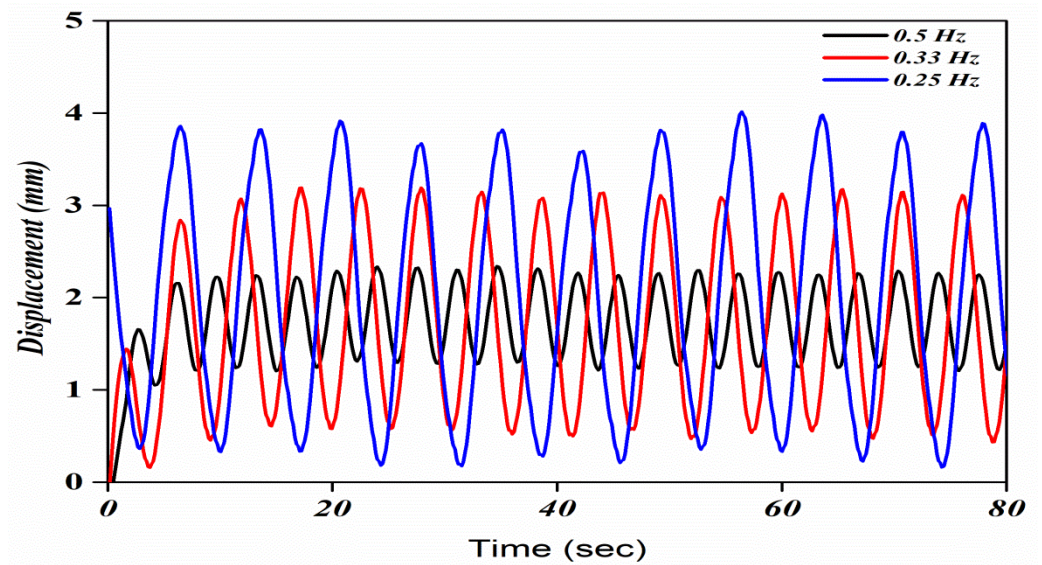
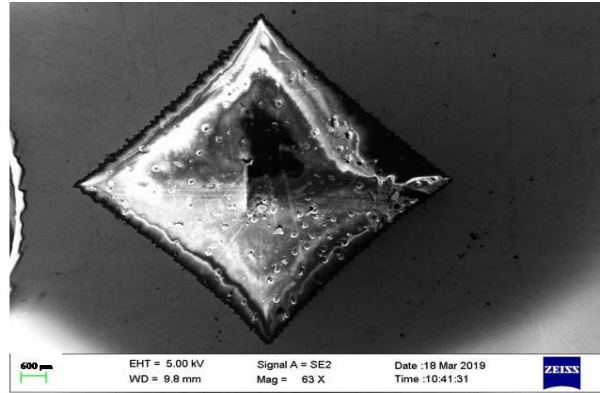


Fig. 28: SEM images of Deltoid pattern and Frequency based displacement vs time graph of Deltoid pattern.

(d) Ladder shape pattern

Fig. (29) shows the SEM images of the Ladder pattern. Investigation of Maximum displacement on the basis of frequency was conducted for the Ladder pattern and it has been observed that the maximum displacement was 0.71, 1.14 and 1.29 in mm at 0.50hz, 0.33hz, and 0.25hz respectively which can be shown by Displacement vs Time graph as shown in Fig(29).

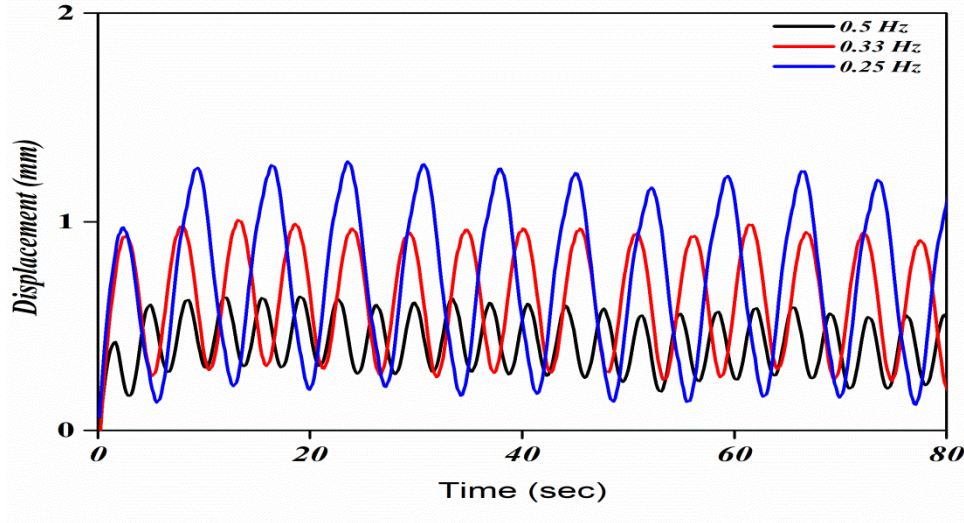
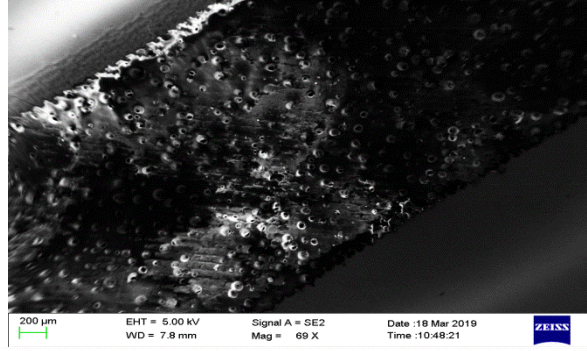


Fig. 29: SEM images of Ladder shaped pattern and Frequency based displacement vs time graph of ladder pattern.

(e) Comb-Shape pattern

Fig(30) shows the SEM images of the Comb-Shaped pattern. Investigation of Maximum displacement on the basis of frequency was conducted for the Comb-Shaped pattern and it has been observed that the maximum displacement was 2.13, 2.68 and 3.52 in mm at 0.50Hz, 0.33Hz, and 0.25Hz respectively which can be shown by Displacement vs Time graph as shown in Fig(30).

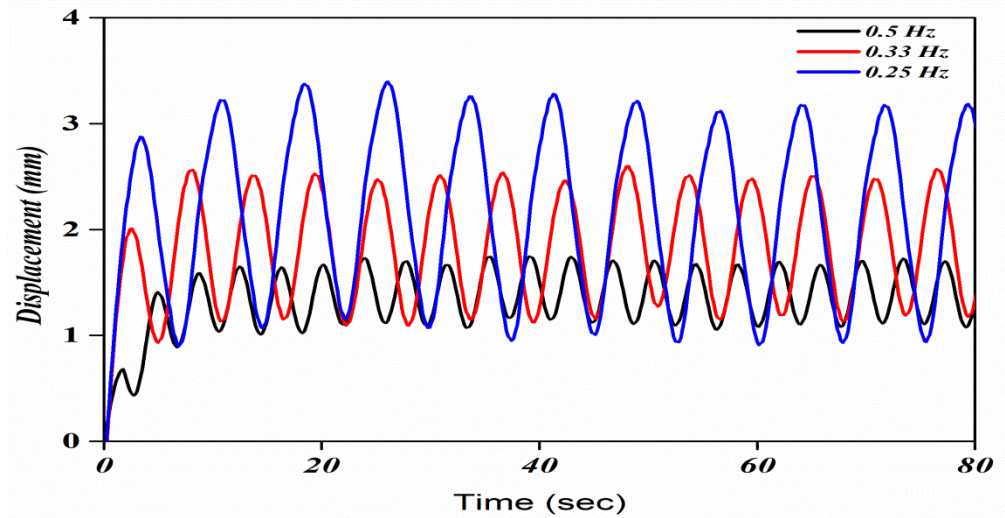
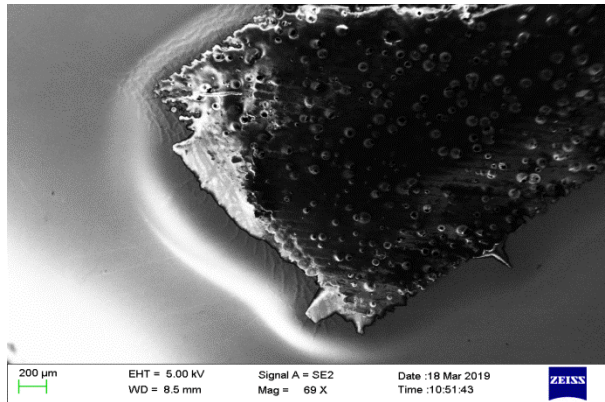


Fig.30: SEM images of Comb-shaped pattern and Frequency based displacement vs time graph of comb-shaped pattern

(f) Fully Deposited

In a planar fully deposited SMA, it was found that the maximum displacement obtained was 1.20,1.89 and 3.33 in mm at 0.50,0.33 and 0.25 Hz respectively whose Displacement vs Time graph can be displayed as shown in Fig. (31).

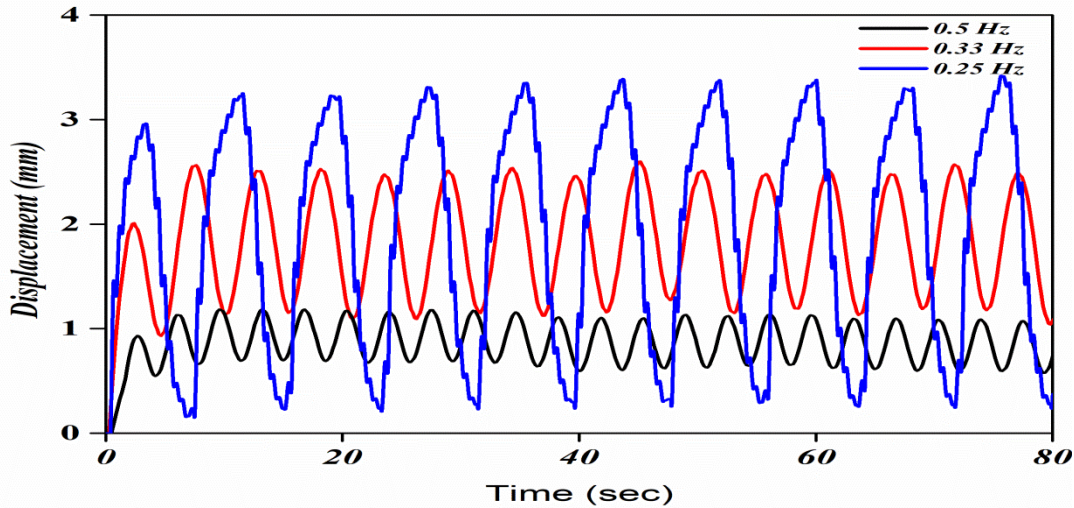
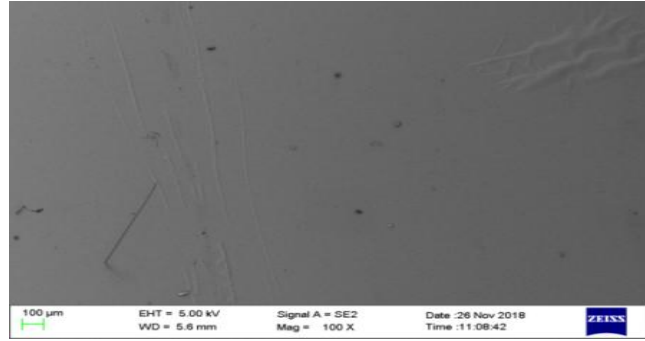


Fig.31: SEM images of Planar Fully Deposited SMA and frequency based displacement vs time graph of Planar Fully Deposited SMA.

4.4.3 COMPARISON OF BREADED SHAPED PATTERN AND COMB SHAPED PATTERN

It has been observed that the maximum displacement obtained in an SMA bimorph of CuAlNi was at 3V and on increasing the voltage further approx. same amount of displacement was obtained in some pattern and some patterns starts burning. So we kept the voltage as a constant and tried to vary the current from 1A to 3A, and observed that most of the pattern gets burnt at a current of 3A and only two patterns i.e. comb-shaped pattern and breaded shaped pattern showed some amount of actuation without getting burnt. On the one hand, the comb-shaped pattern showed a

displacement of about 8.02mm at 3V&3A, on the other hand, the breaded shaped pattern showed a displacement of 7.57mm at 3V&3A. from all of these we can conclude that comb-shaped pattern and breaded shaped pattern can be used for the application of high actuation

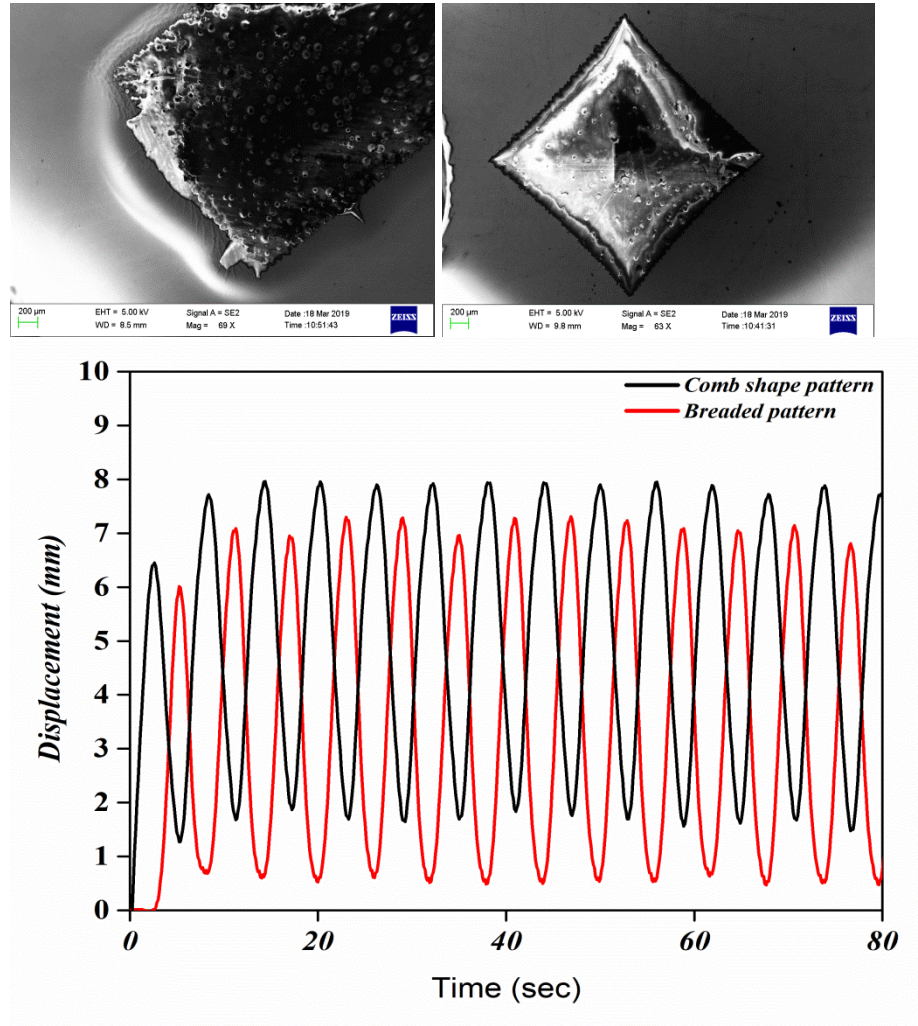


Fig. 32: Displacement vs time graph of Comparison of Comb-shape pattern and breaded shape pattern.

Pattern		Displacement (mm)					
		Circular	Breaded	Deltoid	Ladder	Comb	Without pattern
Voltage	1 V	0.64	0.41	0.50	0.44	0.48	0.54
	2 V	1.54	1.35	3.43	1.20	2.34	1.67
	3 V	2.24	1.58	4.10	1.29	3.52	3.33
Frequency	0.5 Hz	0.90	0.94	2.38	0.71	2.13	1.2
	0.33 Hz	1.82	1.34	3.38	1.14	2.68	1.89
	0.25 Hz	2.24	1.58	4.10	1.29	3.52	3.33
Current	1 A	2.24	1.66	4.10	1.29	3.52	3.33
	3 A	Burnt	7.57	burnt	burnt	8.02	burnt

Table4: Comparison of patterned SMA with Planar Fully Deposited SMA

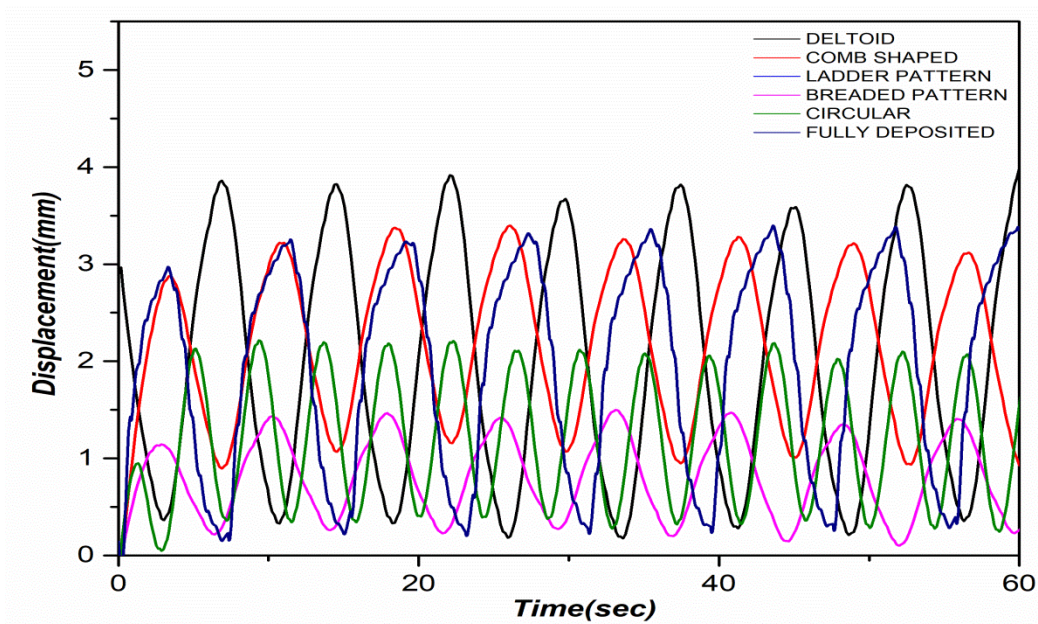


Fig. 33: Displacement vs time graph of planar Fully Deposited SMA and Patterned SMA.

Table(4) demonstrate the complete overview of all bimorphs. On comparison of all the bimorphs, it was concluded that the deltoid pattern is better one among all the patterns because it provides the maximum displacement in comparison to others. Actuation or displacement of the bimorph basically depends on the loads due to deposited material, rate of heat transfer and the flowing of current during electrical actuation. Deltoid pattern gives the maximum displacement of 4.10mm at 3V and 0.25 Hz. On comparing the planar deposited bimorph with all the patterns, it was observed that the Deltoid and Comb-shaped pattern provides more displacement than the bimorph of without pattern but ladder-shaped, breaded shaped and circular pattern gives the lesser displacement. Fig. (33) depicted the time vs displacement graph of different patterns.

Shape Recovery Ratio

Shape recovery ratio is the ratio of the average of bimorph at a specified temperature to the average of bimorph at room temperature. Shape recovery ratio is used to find out the change in curvature of a bimorph at a specified temperature from its curvature at room temperature. In order to examine the shape recovery ratio of CuAlNi deposited bimorph, a substrate heater as shown in Fig. (34) was used. For that, a bimorph was clamped like a butterfly structure with the help of Kapton or thermal tape to a substrate heater and heat was provided to it from room temperature to a temperature where it starts burning and the observation was noted down at a definite interval of temperature, after that cool it down to a room temperature and again observation was noted at that definite interval of temperature. when this observation compared with the room temperature observation then these will show the shape recovery ratio. [22] D_{recovery} value improved on increasing the temperature. On the cooling method, the D_{recovery} value reduced and the initial value was lastly retrieved. This demonstrated the ability of the

developed samples to exhibit two-way shape memory effect, with polyimide acting as a bias force during cooling. Fig. (34) shows the setup of plate heating or substrate heating used to investigate the shape recovery ratio. It is evident that the film deposited on a sheet of polyimide demonstrate sheat cycle two-way movement. It appears that the two-way movement originates in martensitic transformations and their reverse. The movie is at room temperature in the martensitic stage. When heating, the film deposited on a polyimide sheet returns through the inverse conversion, lastly the parent stage is produced entirely.



Fig. 34: Images of Plate Heating Setup for measuring Shape Recovery

$$D_t = (D_1 + D_2) / 2$$

$$D_{\text{recovery}} = D_t / D_{\text{room}}$$

D_1 = Inner diameter of the bimorph

D_2 = Outer diameter of the bimorph

D_t = Average diameter of bimorph at a specified temperature

Ratio.

4.4.4 SHAPE RECOVERY RATIO ANALYSIS

(a) Circular pattern

Fig(35) shows the shape recovery ratio vs temperature curve of a CuAlNi deposited circular pattern. Shape recovery ratio is increased and saturated on the supply(heating) method to a permanent value and retrieved on the interception(cooling) process to its initial value. It has been observed that the maximum D_{recovery} is 1.36 in the circular pattern.

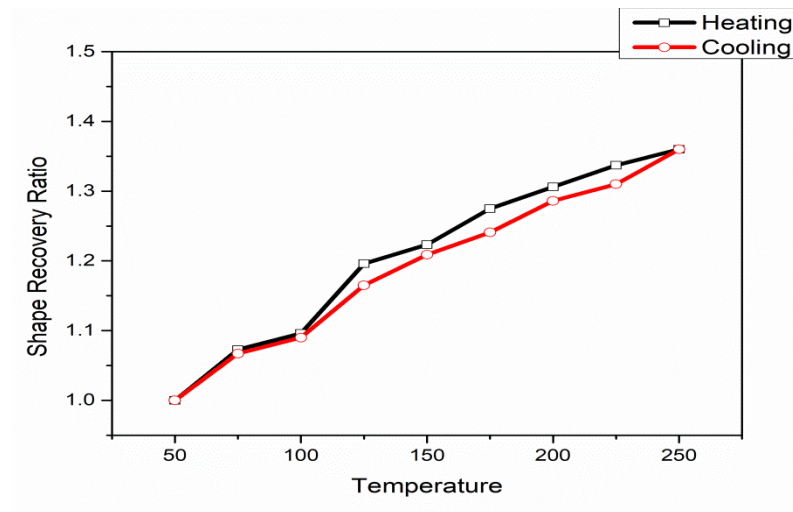
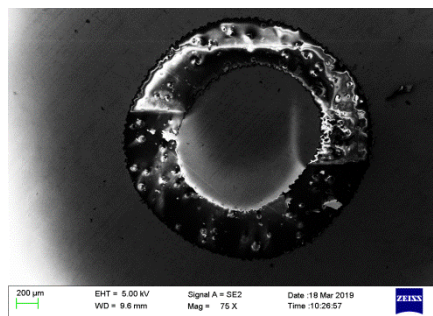


Fig. 35: Temperature vs Shape Recovery Ratio graph of Circular pattern

(b) Ladder pattern

Fig(36) shows the shape recovery ratio vs temperature curve of a CuAlNi deposited ladder pattern. It has been observed that the maximum D_{recovery}

in a ladder pattern was 1.34. In a ladder-shaped pattern, the contact point was reduced due to a number of a closely packed rectangular structure, outcome of which less Shape recovery ratio was obtained.

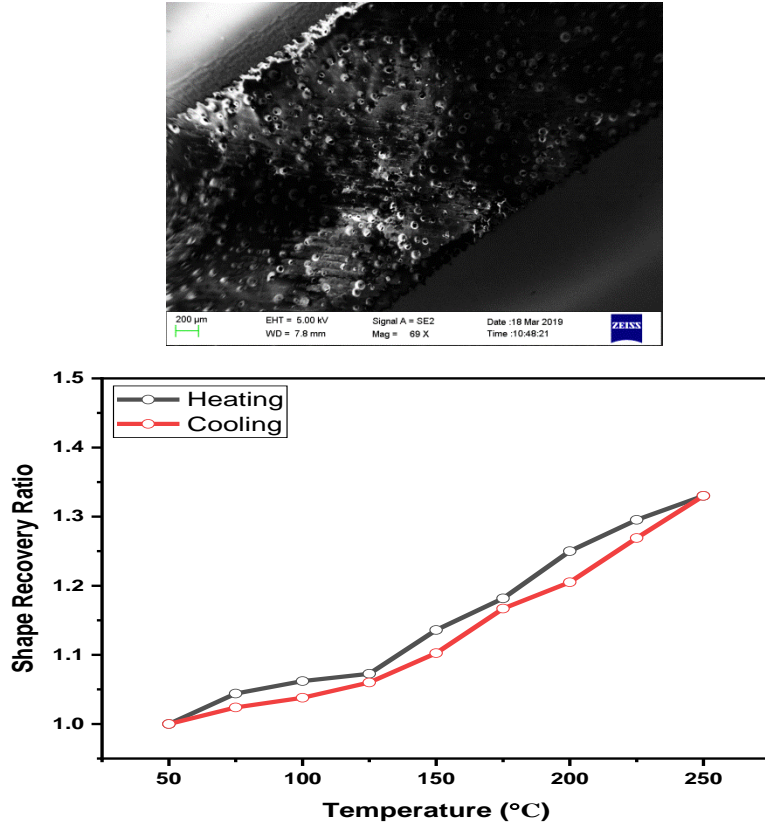


Fig. 36: Temperature vs Shape Recovery Ratio graph of Ladder pattern

(c) Comb-Shaped pattern

Fig(37) shows the shape recovery ratio vs temperature curve of a CuAlNi deposited comb-shaped pattern. In the comb-shaped pattern maximum, D_{recovery} obtained was 1.418. In a comb-shaped pattern, less amount of deposited material was in contact in comparison to fully deposited but more than the other patterns that's why it gives a better outcome than the other patterns.

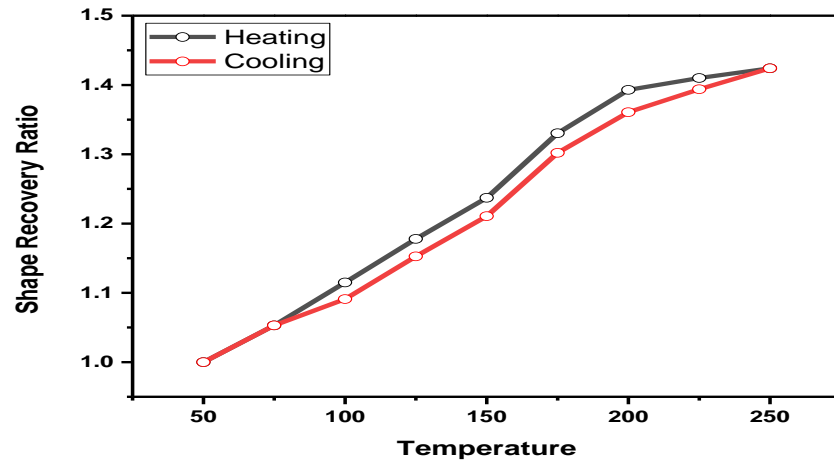
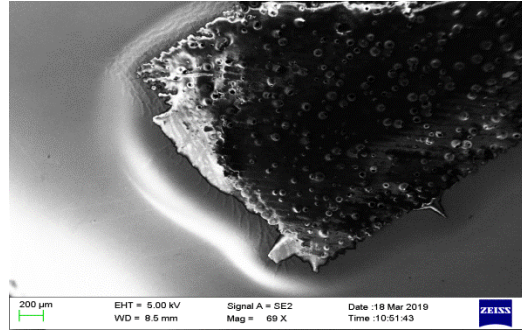


Fig. 37: Temperature vs Shape Recovery Ratio graph of Comb-Shaped Pattern

(d) Breaded shaped pattern

Fig(38) shows the shape recovery ratio vs temperature curve of a CuAlNi deposited breaded-shaped pattern. In the breaded-shaped pattern maximum, D_{recovery} obtained was 1.248.

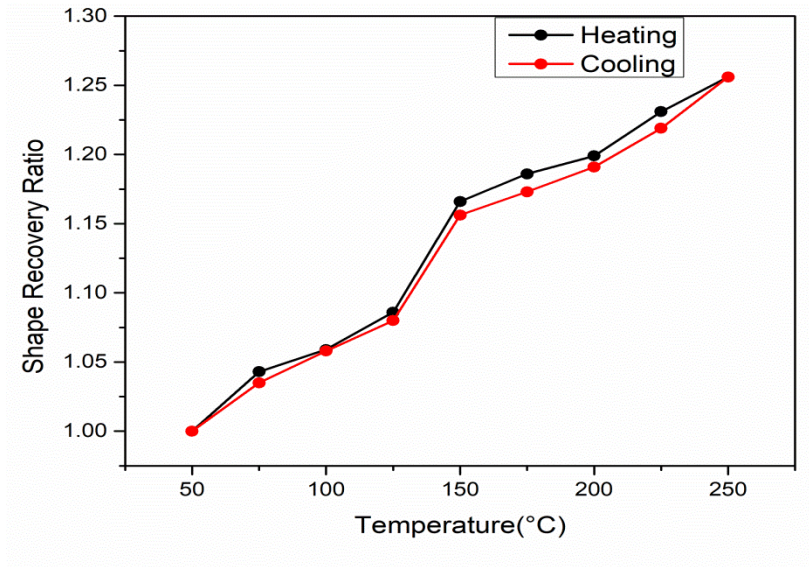
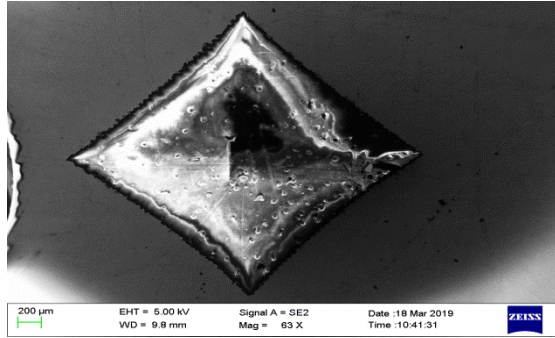


Fig. 38: Temperature vs Shape Recovery Ratio graph of Braided-Shape Pattern

(e) Fully Deposited

Fig. (39) shows the shape recovery ratio vs temperature curve of a CuAlNi deposited bimorph. In the comb-shaped pattern maximum, D_{recovery} obtained was 1.656. Point of contact plays an important role in the shape recovery ratio. Most of the deposited portion was in contact in fully deposited bimorph, thus providing the highest retrieval percentage of shape among all bimorph.

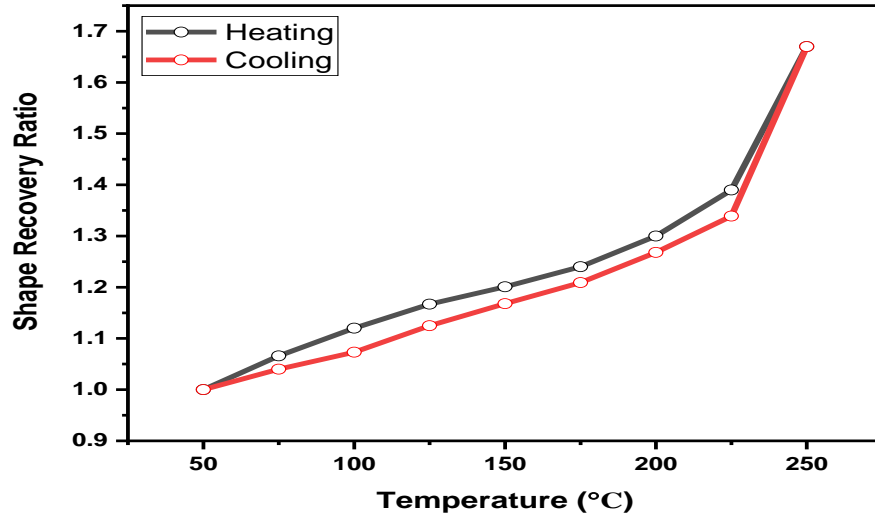
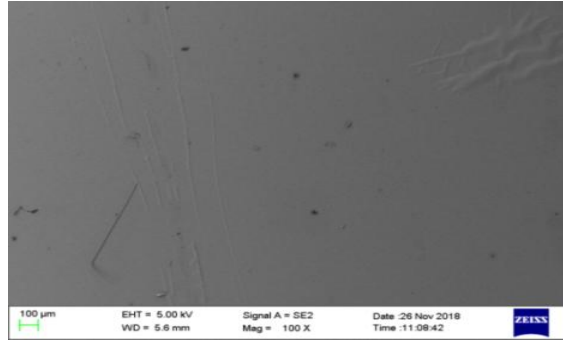


Fig. 39: Temperature vs Shape Recovery Ratio graph of Planar Fully Deposited.

4.4.5 Differential scanning calorimetry

Differential Scanning Calorimetry or DSC is a thermoanalytical method in which the difference in the quantity of heat needed to raise a sample's temperature and reference is measured as a function of temperature[23]. Throughout the experiment, the sample and reference are retained at almost the same temperature. From experimentation, it was observed that the Austenitic start temperature A_s and Austenitic Finish Temperature A_f was found to be 233.2°C and 234.5°C respectively and Martensitic start temperature M_s and Martensitic Finish temperature M_f was observed to be 217.5°C and 216.3°C respectively.

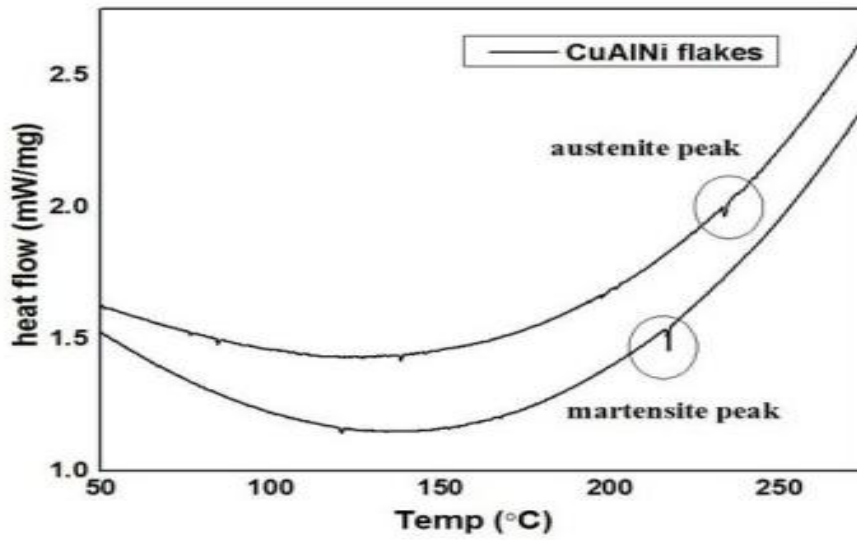


Fig. 40: Temperature vs Heat flow graph of CuAlNi

Phase	Temperature (Degree Centigrade)
Austenite Start Temperature (A_s)	233.2
Austenite Finish Temperature (A_f)	234.5
Martensite Start Temperature (M_s)	217.5
Martensite Finish Temperature (M_f)	216.3

Table 5:Phase Transformation of CuAlNi

4.4.6 Measurement of thickness

A Contact type profilometer was used to investigate the thickness of the coating of deposited CuAlNi over the Kapton polyimide substrate. A contact type probe used for the measurement of thickness and it was observed $0.73\mu\text{m}$ deposited on the Kapton polyimide substrate.

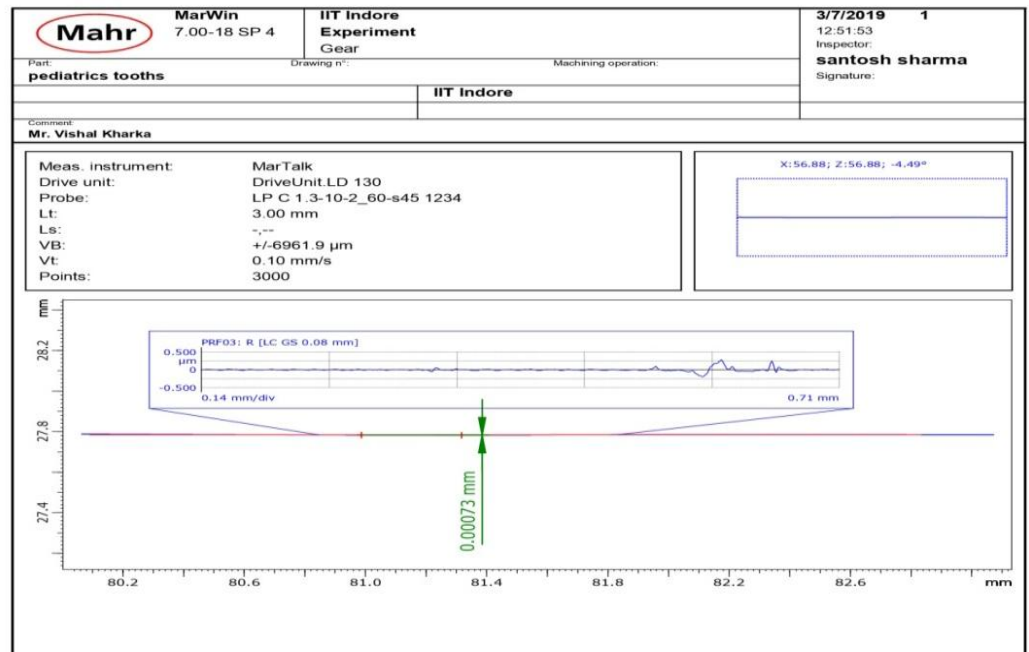


Fig. 41: Image showing the thickness of CuAlNi Bimorph

4.4.7 ENERGY DISPERSIVE X-RAY SPECTROSCOPY

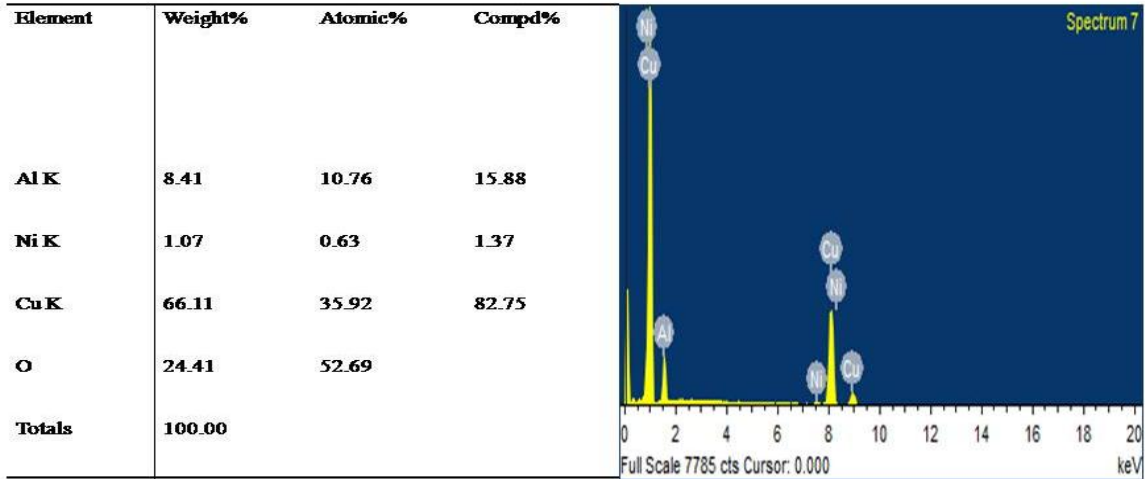


Table 6: Composition analysis results obtained from EDX analysis

Summary

This chapter deals with the Results and discussions of the bimorph and comparison of fully deposited planar bimorph with the patterned bimorph which can be summarized as follow:

- Laser fabrication was the best method for patterning on the planar fully deposited bimorph.
- Deltoid pattern was the best pattern among all the pattern as it provides the maximum displacement of 4.12mm at 3V.
- Deposited material can be easily removed by using a proper laser parameter of Ytterbium-doped laser (i.e. 1064 nm,300mm SOD,20W & Single Pass) from the planar fully deposited bimorph.
- Comb-shaped pattern and Deltoid pattern provides better maximum displacement than the planar fully deposited bimorph.
- SEM images of patterned bimorph shows the proper adhesion.
- $A_s, A_f, M_s \& M_f$ found to be 233.2 and 234.5, 217.5 and 216.3 in °C respectively measured by DSC.

CHAPTER 5

CONCLUSION AND FUTURE SCOPE

The main aim of this thesis is to create a pattern on a planar fully deposited thin film in Kapton polyimide sheet and the comparison of its displacement with the planar fully deposited thin film in a Kapton polyimide sheet. From Observation, it was investigated that the displacement or actuation during electrical actuation was depended on the path of current flow throughout the deposition and the total load on it during actuation. Through the experimentation, it was observed that on creating a pattern in a bimorph, total load on it gets reduced on account of the removal of deposited material, but some time due to the improper path of the current flow, it provides less displacement in comparison to the planar fully deposited pattern (having more load). The complete results are summarized as;

- Deposition should be at a very high vacuum of 0.05mbar in a Kapton polyimide substrate.
- Laser fabrication is the best way for creating a pattern in a planar fully deposited thin film.
- Deposited material of 0.79 μm from the Kapton polyimide substrate can be removed by using a proper laser parameter of Ytterbium-doped laser (i.e. 1064 nm,300mm SOD,20W & Single Pass)
- Displacement or actuation is mostly dependent on the load on a bimorph and the flow of current during electrical actuation.
- Deltoid pattern was the best pattern among all the pattern as it provides the maximum displacement of 4.12mm at 3V.
- Comb-shaped pattern and Deltoid pattern provides better maximum displacement than the planar fully deposited bimorph.

- SEM images display the proper adhesion of the continuous film.
- The Austenite start temperature A_s and Austenite finish temperature A_f was found to be 233.2 and 234.5 in °C respectively measured by DSC.
- The Martensite start temperature M_s and Martensite finish temperature M_f was found to be 217.5 and 216.3 in °C respectively measured by DSC.

FUTURE SCOPE

Present work comprises of comparison of planar fully deposited bimorph with the patterned deposited bimorph. The main aim of this work was to increase the actuation or displacement by patterning on fully deposited planar bimorph.

- There is a possibility of increasing the displacement by using a different type of patterning on fully deposited planar bimorph.
- Micro Bird can be designed by using bimorph in place of the wing which can be used as a spycam.
- Different displacement can be obtained in a distinct pattern at a single voltage which can be used as an application.

CHAPTER 6

Reference

- [1] Dimitris_C_Lagoudas, *[Dimitris_C_Lagoudas(2007)]_Shape_memory_alloys__modeling.pdf*. 2007.
- [2] Y. Fu, H. Du, W. Huang, S. Zhang, and M. Hu, “TiNi-based thin films in MEMS applications: A review,” *Sensors Actuators, A Phys.*, vol. 112, no. 2–3, pp. 395–408, 2004.
- [3] E. Makino, T. Mitsuya, and T. Shibata, “Fabrication of TiNi shape memory micropump,” *Sensors Actuators, A Phys.*, vol. 88, no. 3, pp. 256–262, 2001.
- [4] N. Choudhary and D. Kaur, “Shape memory alloy thin films and heterostructures for MEMS applications: A review,” *Sensors Actuators, A Phys.*, vol. 242, pp. 162–181, 2016.
- [5] I. F. Ü. R. H. Mikrosystemtechnik, “Thin-Film Shape-Memory Alloy Actuated Mircopumps,” vol. 7, no. November, pp. 245–251, 2016.
- [6] L. C. Brinson, “One-dimensional constitutive behavior of shape memory alloys: Thermomechanical derivation with non-constant material functions and redefined martensite internal variable,” *J. Intell. Mater. Syst. Struct.*, vol. 4, no. 2, pp. 229–242, 1993.
- [7] L. Sun and W. M. Huang, “Nature of the multistage transformation in shape memory alloys upon heating,” *Met. Sci. Heat Treat.*, vol. 51, no. 11–12, pp. 573–578, 2009.
- [8] I. Mihálcz, “Fundamental characteristics and design method for nickel-titanium shape memory alloy,” *Period. Polytech. Mech. Eng.*, vol. 45, no. 1, pp. 75–86, 2001.
- [9] D. J. Hartl, G. Chatzigeorgiou, and D. C. Lagoudas, “Three-dimensional modeling and numerical analysis of rate-dependent irrecoverable deformation in shape memory alloys,” *Int. J. Plast.*, vol. 26, no. 10, pp. 1485–1507, 2010.
- [10] N. Marin and Y. Serruys, “Under and Out of Irradiation,” vol. 5, pp. 175–180, 1995.
- [11] A. Ishida and M. Sato, “Development of Polyimide/SMA Thin-Film Actuator,” *Mater. Sci. Forum*, vol. 654–656, pp. 2075–2078, 2010.

- [12] K. Akash, A. K. Shukla, S. S. Mani Prabu, D. C. Narayane, S. Kanmanisubbu, and I. A. Palani, "Parametric investigations to enhance the thermomechanical properties of CuAlNi shape memory alloy Bi-morph," *J. Alloys Compd.*, vol. 720, pp. 264–271, 2017.
- [13] F. C. Lovey, A. M. Condó, J. Guimpel, and M. J. Yacamán, "Shape memory effect in thin films of a Cu-Al-Ni alloy," *Mater. Sci. Eng. A*, vol. 481–482, no. 1-2 C, pp. 426–430, 2008.
- [14] K. Akash *et al.*, "Investigations on actuation characteristics and life cycle behaviour of CuAlNiMn shape memory alloy bimorph towards flappers for aerial robots," *Mater. Des.*, vol. 144, pp. 64–71, 2018.
- [15] Y. Jeong, J. K. Sahu, D. N. Payne, and J. Nilsson, "Ytterbium-doped large-core fibre laser with 1 kW of continuous-wave output power," *Trans. Korean Inst. Electr. Eng.*, vol. 57, no. 6, pp. 982–984, 2008.
- [16] D. Erickson, D. Sinton, and D. Li, "Joule heating and heat transfer in poly(dimethylsiloxane) microfluidic systems," *Lab Chip*, vol. 3, no. 3, pp. 141–149, 2003.
- [17] K. Mori, J. Li, A. Roytburd, and M. Wuttig, "Patterned Shape Memory Alloy Films," *Mater. Trans.*, vol. 43, no. 5, pp. 951–955, 2005.
- [18] K. Reichelt and X. Jiang, "The preparation of thin films by physical vapour deposition methods," *Thin Solid Films*, vol. 191, no. 1, pp. 91–126, 1990.
- [19] C. Schick, "Differential scanning calorimetry (DSC) of semicrystalline polymers.," *Anal. Bioanal. Chem.*, vol. 395, no. 6, pp. 1589–611, 2009.
- [20] S. Fähler and H. U. Krebs, "Calculations and experiments of material removal and kinetic energy during pulsed laser ablation of metals," *Appl. Surf. Sci.*, vol. 96–98, no. 95, pp. 61–65, 1996.
- [21] N. M. Bulgakova, R. Stoian, A. Rosenfeld, I. V. Hertel, and E. E. B. Campbell, "Electronic transport and consequences for material removal in ultrafast pulsed laser ablation of materials," *Phys. Rev. B - Condens. Matter Mater. Phys.*, vol. 69, no. 5, pp. 1–12, 2004.
- [22] Y. Kishi, N. Ikenaga, N. Sakudo, and Z. Yajima, "Shape memory behavior of TiNi alloy films sputter-deposited on polyimide substrate," *J. Alloys Compd.*, vol. 577, no. SUPPL. 1, pp. S210–S214, 2013.

- [23] V. Recarte, J. I. Pérez-Landazábal, A. Ibarra, M. L. Nó, and J. San Juan, "High temperature β phase decomposition process in a Cu-Al-Ni shape memory alloy," *Mater. Sci. Eng. A*, vol. 378, no. 1-2 SPEC. ISS., pp. 238–242, 2004.
- [25] ASM International. Handbook Committee (Ed.). (1990). *Properties and selection: nonferrous alloys and special-purpose materials* (Vol. 2). Asm Intl.
- [26] M. Gojić, L. Vrsalović, S. Kožuh, A. Kneissl, I. Anžel, S. Gudić, B. Kosec, M. Kliškić, Electrochemical and microstructural study of Cu-Al-Ni shape memory alloy, *J. Alloys Compd.* 509 (2011) 9782–9790. doi:10.1016/j.jallcom.2011.07.107.
- [27] V. Sampath, Studies on the effect of grain refinement and thermal processing on shape memory characteristics of Cu–Al–Ni alloys, *Smart Mater. Struct.* 14 (2005) S253–S260. doi:10.1088/0964-1726/14/5/013.
- [28] Henderson, R., & Schulmeister, K. (2003). *Laser safety*. CRC Press.
- [29] Otsuka, K., & Wayman, C. M. (Eds.). (1999). *Shape memory materials*. Cambridge university press.
- [30] Duerig, T. W., Melton, K. N., & Stöckel, D. (2013). *Engineering aspects of shape memory alloys*. Butterworth-Heinemann.
- [31] Lee, D. H., & Cho, N. G. (2012). Assessment of surface profile data acquired by a stylus profilometer. *Measurement science and technology*, 23(10), 105601.
- [32] https://www.google.com/search?q=kapton+polyimide+sheet&safe=off&rlz=1C1CHBD_enIN805IN805&source=lnms&tbn=isch&sa=X&ved=0ahUKEwjuy6PDyfriAhWIpI8KHQrrDg4Q_AUIECgB&biw=1366&bih=657#imgrc=uwapLR_UWNFULM:

